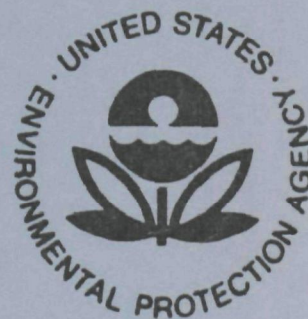


EPA-650/2-73-008

October 1973

Environmental Protection Technology Series

**DEVELOPMENT OF A SUPPLEMENTARY
EMISSION MEASUREMENTS
MONITORING SYSTEM**



DEVELOPMENT OF A SUPPLEMENTARY EMISSION MEASUREMENTS MONITORING SYSTEM

by

Paul F. Bennewitz

Thunder Scientific Corporation
623 Wyoming S. E.
Albuquerque, New Mexico 87123

Contract No. 68-02-0588
Program Element No. 1A1010

EPA Project Officer: Fredric C. Jaye

Chemistry and Physics Laboratory
National Environmental Research Center
Research Triangle Park, North Carolina 27711

Prepared for

OFFICE OF RESEARCH AND DEVELOPMENT
U. S. ENVIRONMENTAL PROTECTION AGENCY
WASHINGTON, D.C. 20460

October 1973

This report has been reviewed by the Environmental Protection Agency and approved for publication. Approval does not signify that the contents necessarily reflect the views and policies of the Agency, nor does mention of trade names or commercial products constitute endorsement or recommendation for use.

TABLE OF CONTENTS

| | |
|---|----|
| Abstract | 1 |
| Objective | 11 |
| Scope | 1 |
| Introduction | 2 |
| Interstitial sensing | 3 |
| Technical discussion | 4 |
| Fig. 1, Density states three dimensional lattice | 5 |
| Fig. 2, Cutaway ILS Array | 6 |
| Fig. 3, Frequency Vs wave vector | 7 |
| Defect Structure | 8 |
| Fig. 4, Replacement lattice . . . | 9 |
| Ligand Field Theory | 11 |
| Fig. 5, Standing wave, defects . | 12 |
| Fig. 6, H ₂ O Molecule | 13 |
| Fig. 7, Far infrared stretching frequencies | 14 |
| CO, CO ₂ , O ₂ , H ₂ O | 15 |
| Material Selection | 16 |
| Material Analysis | 17 |
| Group Selection, Sensor firing and construction | 18 |
| Test System Configuration | 19 |
| Fig. 8, Block Diagram EMMS . . . | 20 |
| Fig. 9, CO ₂ Gas Sensor | 21 |
| Fig.10, Steam test | 21 |
| Fig.11, Test Unit #7 | 23 |
| Fig.12, Test Unit #5 | 24 |
| Fig.13, Signal conditioning . . . | 25 |
| O ₂ , H ₂ O Sensor | 26 |
| Fig.14, Test Unit #6, calibration | 27 |
| Fig.15, Test Unit #6, | 28 |
| Fig.16, Test Unit #5, steam . . . | 29 |
| Fig.17, Test Unit #5, steam . . . | 30 |
| Life Tests | 31 |
| System Components | 32 |
| Fig.18, WSIS-1000, BR-101R . . . | 33 |
| Fig.19, Gas Sampling System . . . | 34 |
| Bottom, top view | |
| Fig.20, System, front panel and . | 35 |
| Control panel | |
| Fig.21, Atmospheric system and . | 36 |
| Test chamber | |
| Conclusion | 38 |
| Fig. 22, Flow Chart | 39 |
| Fig. 23, System Gas Flow | 40 |
| References | 41 |

ABSTRACT

A prototype Supplementary Emission Measurements System was designed and developed to provide measurement of CO_2 , CO , H_2O , and O_2 in stack gases of stationary emission sources.

Sensors were developed or obtained from other sources to meet the criteria set forth in the requirement.

The system was designed to facilitate direct readout of all channels via individual analog metering. In addition, outputs of 0 to 1 VDC were provided for on-line computer feed.

The system was equipped with a stack sampling probe, filters and pump to provide full and complete stack sampling and measurement capability.

OBJECTIVES AND/OR BACKGROUND

The project for development of a Supplementary Emission Measurements Monitoring System was organized with the following design goals and objectives:

- 1) Design a prototype subsidiary emissions measurements system to measure CO₂, CO, H₂O and O₂ in stack emission gases.

Ranges Requested:

| | | | |
|------------------|-----------------|--------|---------------------|
| CO ₂ | 0 - 20% | - 0.5% | minimum sensitivity |
| CO | 0 - 5% | - 0.1% | " " |
| H ₂ O | 0 - 20% | - 0.5% | " " |
| O ₂ | 0 - 7%, 0 - 22% | | |

- 2) To procure or develop sensor with the specified typical minimum ranges and sensitivities.
- 3) To supply flow velocity of 20 to 120 feet per second.
- 4) To supply temperature measurement in the range of 50° to 700°F.
- 5) To equip the system as required with sampling probes, filters, pump, etc.
- 6) To supply analog meter readouts and simultaneous analog 0 - 1 volt outputs for all parameters.
- 7) To equip the system with suitable zero and calibration circuitry as required.

Report of Development of a
Supplementary Emission Measurements
Monitoring System

SCOPE

This report describes sensors and systems developed to provide precise measurements and readout of subsidiary emissions consisting of CO₂, CO, H₂O and O₂ as required by the Environmental Protection Agency.

Unique methods were implemented which, due to past developmental experience at Thunder Scientific Corporation, were considered to be an advance of the state-of-the-art and highly applicable to the requirement.

Sensing Elements (Solid-State)

This report describes the use of various types of semiconductor materials for discriminatory sensing of various pollutant gases; a superior and unique semiconductor method was used, based upon prior experience gained in the recent development by Thunder Scientific of the advanced state-of-the-art Brady Array bulk-effect humidity sensor. It has been determined that the Brady Array is most effective, accurate and reliable because of its interstitial lattice method of sensing.

Known monocrystalline semiconductors in chip form, when connected to appropriate circuitry via applied electrodes, exhibit various characteristics relative to sensitivity to the environment and various gases, particularly to H₂O in various concentrations; however, not without degradation and irreversible effects to be discussed later. The consensus of opinion in both the past and present has been to assume that when designing a new sensor, for example a humidity sensor, or other types, one should rely upon various effects of different types of materials to achieve the end result, with little thought given to designing specifically to the requirement. Previous sensors, such as those designed for measurement of moisture or relative humidity, relied upon surface phenomenon to achieve a measurement. Desiccants or hygroscopic materials have been heavily relied upon as attractants for moisture for

measurement. If observed under high magnification, all the above configurations may be seen to be agglomerating water or forming islands of moisture during the process of measurement. This means loss of response time and other characteristics leading to undesirable results. Also, because the surfaces of these devices are limited in area, dynamic range is very narrow.

In the case of the Brady Array, humidity sensor, a semiconductor bulk-effect device was constructed which could be proven mathematically to be electrically neutral. A method was discovered in the process of development which allows the construction of microminiature lattice arrays made up of many crystal semiconductor junctions, separated by interstitial spaces. These junctions, estimated to number a million or more, present a very large geometric area, if all crystal faces were spread out side by side. Because the water molecule is extremely small, and the structure is electrically neutral, the molecules may drift randomly and freely into and out of the structure, causing interaction within the semiconductor structure which stresses bonds and changes the volumetric resistance when percent relative humidity or molecular density is changed. Because of the semiconductor nature and the array effect of the structure, the sensor exhibits a near one-to-one ratio in output voltage vs. input excitation as the surrounding moisture or molecular density is changed.

It is this method of approach, the interstitial lattice sensing method (ILS), which was used extensively throughout the requirement.

Introduction

In the following technical discussion, reference will be made periodically to the interstitial lattice method of sensing as applied to a semiconductor-type bulk-effect sensor. This method and the processes involved are proprietary, with patents obtained or in process, having been solely developed by Thunder Scientific during in-house funded R&D programs recently completed, to conceive, develop and construct an advanced state-of-the-art humidity sensor, which is a solid-state bulk-effect semiconductor device. This sensor, designated the Brady Array, is presently being marketed along with signal conditioning modules also developed at Thunder Scientific, with excellent results.

Interstitial Sensing

Interstitial lattice sensing (ILS) is a method wherein an extremely complex crystal array is processed and constructed within a diffusion type furnace. Contrary to normally known configurations of semiconductors where the semiconductor is a monocrystalline structure or die consisting of a single slice cut and diced from a single zone-grown crystal, the interstitial lattice array, measuring only 10 mils in diameter and 100 mils in length, consists of thousands of semiconductor junctions preformed and processed so as to provide interstitial bulk access to all faces of the crystal lattices and junctions within the structure. Thus, single molecules of various gases and constituents may easily drift into and out of the array, creating Fermi-related energy exchanges, causing the bonds within the lattices to be stressed. Because they are vibrating at a discrete and synonymous stretching frequency with the impressed molecular field, energy is released within the structure to the free electrons therein, which causes a shift of the Fermi level, thus causing a change in the volumetric resistance of the structure (see Figure 2).

Appropriate signal conditioning, generating an excitation voltage in a simple bridge arrangement and a demodulator for conversion of the signal to direct current, thus supplies an output signal across an output termination proportional to the phenomena, for analysis by direct reading end instruments or computer manipulation.

Greater Sensing Area vs. Size

The crystal lattice array, sensing by interstitial means, provides a sensor area, when viewed at a molecular level, hundreds of magnitudes greater than that provided by a monocrystalline semiconductor. Rather than presenting one or a few semiconductor junctions to the medium, which subsequently will greatly limit the dynamic range of readout, the ILS presents a large geometric area if all crystal faces and junctions were laid out side by side. Therefore, dynamic ranges of many orders of magnitude become available. This is a major asset when dealing with units of measurement such as those related to pollution and contaminant levels, i.e., PPHM, PPM, %, mass, etc.

Technical Discussion

In a monocrystalline semiconductor, great care is taken to prevent the influx of, or contamination by, impurities, both in the processing environment and following packaging. For example, the use of SiO_2 in the field electrode of MOS transistors has caused difficulties, since this glass easily absorbs foreign ions that can move under field influence through the glass. Thus sodium ions can easily move within the glass if outside fields are applied, and therefore, a change in conductivity and dielectric constant causes a change in impedance and capacity values. Other impurity atoms such as CO , HCL and HF can possibly move through the glass, causing permanent changes in impedance and capacity.

At first glance, one would tend to assume that because of these phenomena, monocrystalline semiconductors could be used directly to detect these impurities; however, this is not entirely true. The prime reason in this instance, whether the monocrystalline semiconductor is SiO_2 or Ge or combinations or with various dopants, is that the principal of operation must be based upon a theory of absorption or adsorption, such as in the previously mentioned surface-type humidity sensors, thus narrowing the dynamic range and creating major problems of repeatability and reproducibility.

Of key and significant importance and one of the most major disadvantages which should not be overlooked in evaluation of devices suggesting monocrystalline structures, is that these structures, solely by the fact that they are monocrystalline, are highly susceptible to doping, even in limited amounts. All the various gases concerning in this report and most others indicated in the references are "dopants". These dopants cause irreversible changes of impedance, capacitance and resistance within monocrystalline structures. These changes are a major source of inaccurate, unreliable devices for the purpose intended.

Interstitial lattice sensing (ILS) and the crystal lattice array represent an advancement in the "state-of-the-art", based upon the past two years of research carried on at Thunder Scientific Corporation. This array is a semiconductor device that does lend itself directly to sensing of the various parameters required. The ILS device can be thought of, in one sense, as a cross between an amorphous semiconductor and a monocrystalline semiconductor, i.e., the

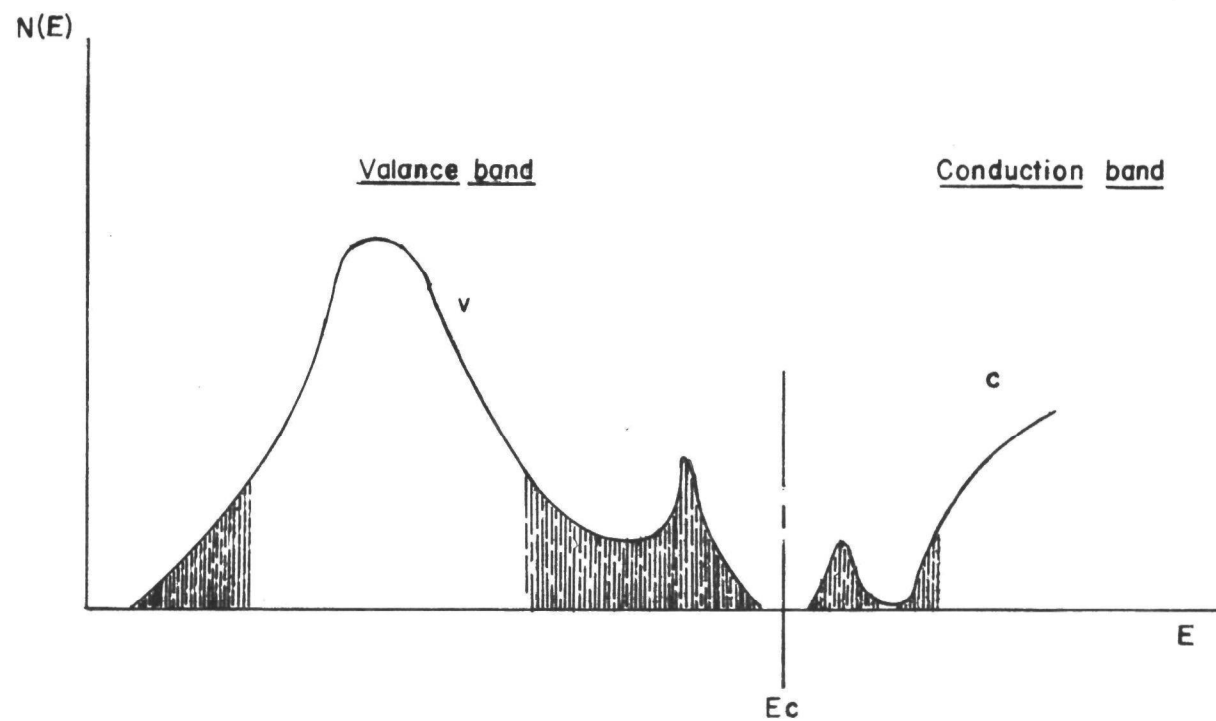


FIGURE ONE
DENSITY STATES THREE DIMENSIONAL
LATTICE

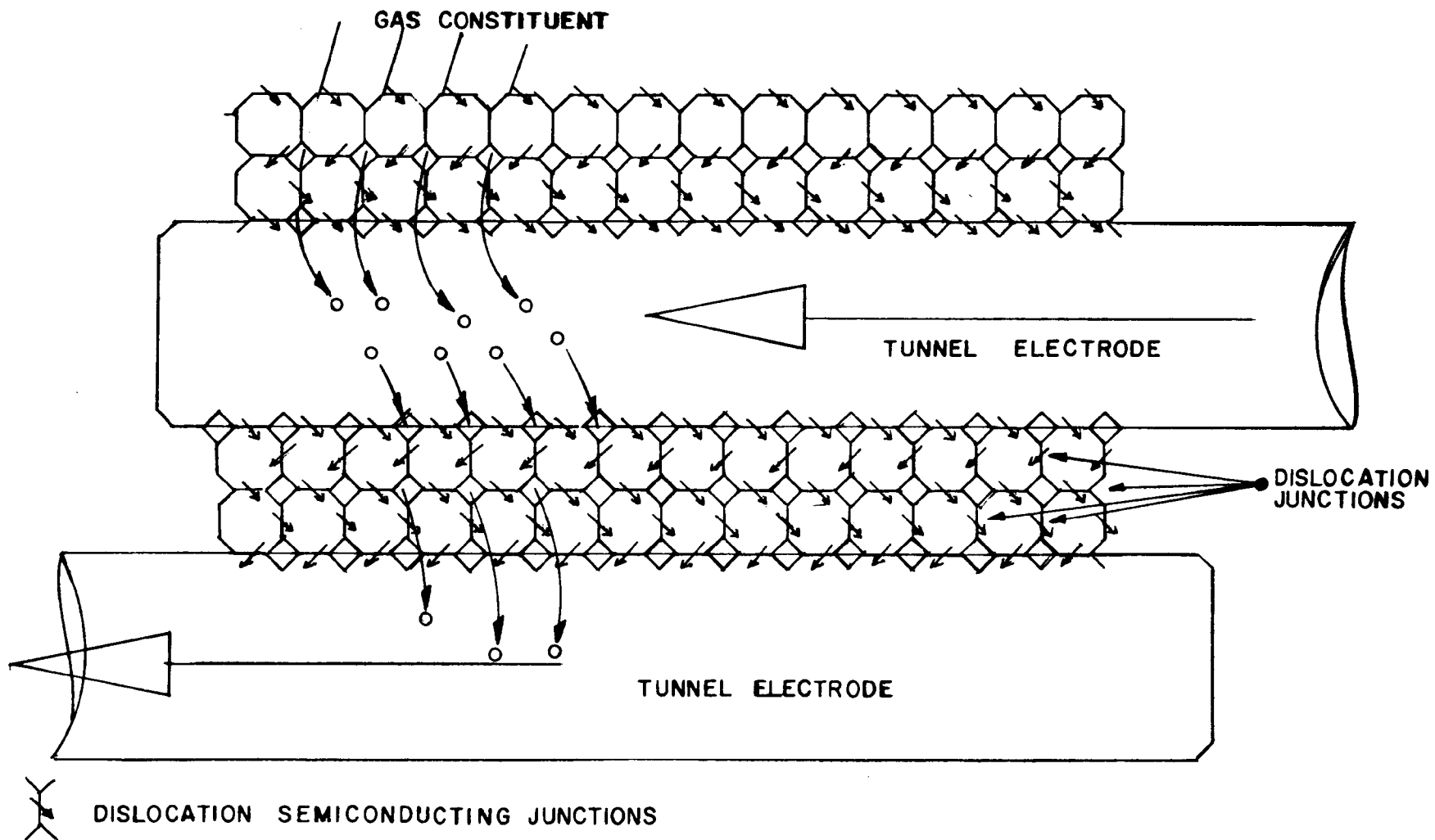


FIGURE TWO
CUTAWAY ILS ARRAY

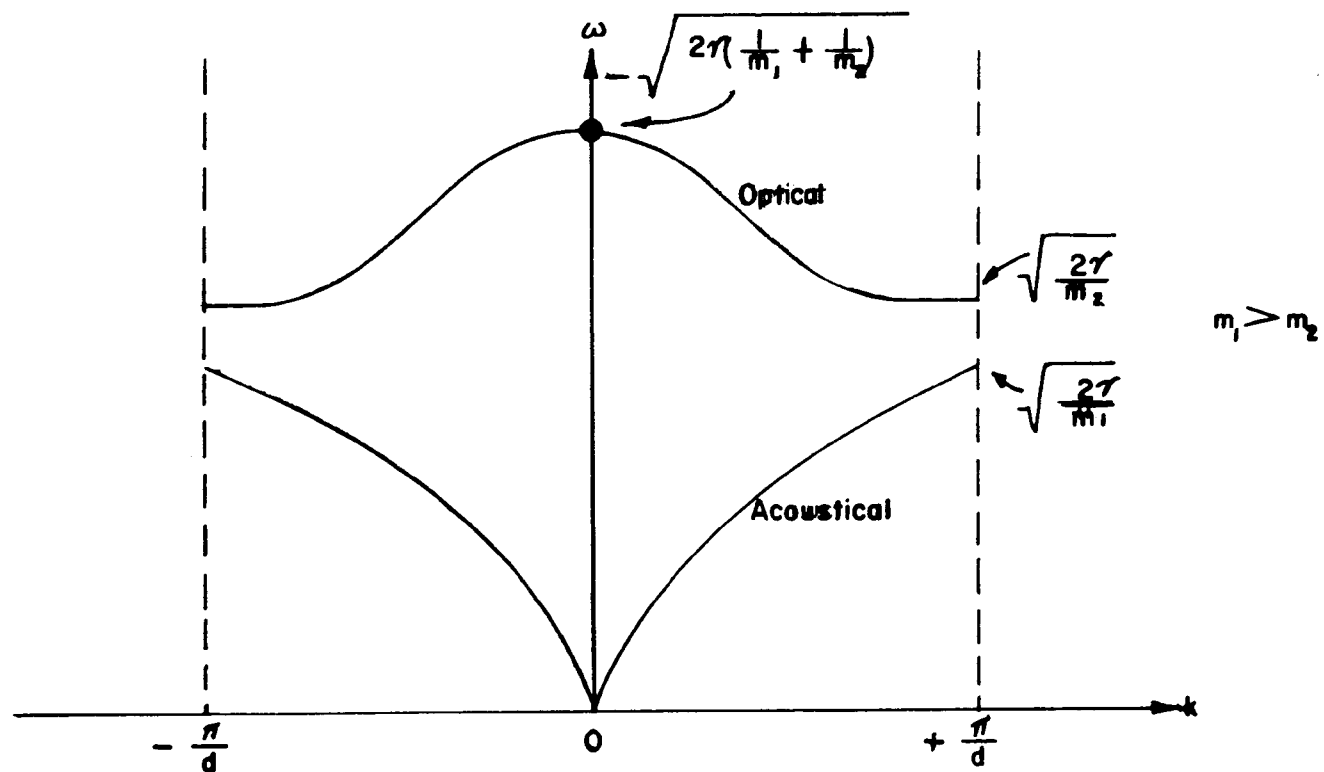


FIGURE THREE
FREQUENCY Vs WAVE VECTOR

electronic properties of defects of the dislocation type play a somewhat important part, yet the structure is polycrystalline while at the same time being deliberately highly disordered.

This disordering accounts for the large interstitial areas, most important when sensing gas constituents such as H_2O , CO , CO_2 , etc. In effect, the gas tends to behave like and may be treated as electron gas. Therefore, in analysis, one may derive from measurements of temperature dependence, resistance, thermo-electric power and reflectivity, that this type of structure is far less sensitive to doping than either amorphous or monocrystalline structures.

In any crystal, monocrystal, or the individual disordered mode crystals of the ILS structure, two different vibrational modes exist, which can be related by:

$$\omega^2 = \left(\frac{1}{m_1} + \frac{1}{m_2} \right) \pm \left[\left(\frac{1}{m_1} + \frac{1}{m_2} \right) - \frac{4 \sin^2 Kd}{m_1 m_2} \right]^{1/2}$$

These two vibrational modes are of great importance in real lattices giving the value for ω at the limits (see figure 3). Since the lower function corresponds to in-phase movement of nearest neighbors (odd and even numbered atoms), it is called the "acoustical" branch, because the lower frequencies generated in this kind of excitation correspond to the acoustical range for most crystals. The upper branch, shown in figure 3, is called the optical branch, because these frequencies belong in the electromagnetic infrared frequency range. It is these phenomena and characteristics, among others to be explained, which account for the prime theory of the ILS array. The frequency vs. wave-number functions in figure 3 can have different bands if more than two different particle masses or more than two force constants are involved. The main difference between their frequency range remains the cophase or contraphase movement of nearest neighbors.

Defect Structure

Contrary to the case of monocrystalline semiconductors where it is desired to hold point defects to a bare minimum, in the ILS structure, the opposite is the case. Defects within the structure are of absolute necessity in conjunction with the disordered array for operation of the system. For example, in looking at the periodic structure in the simple

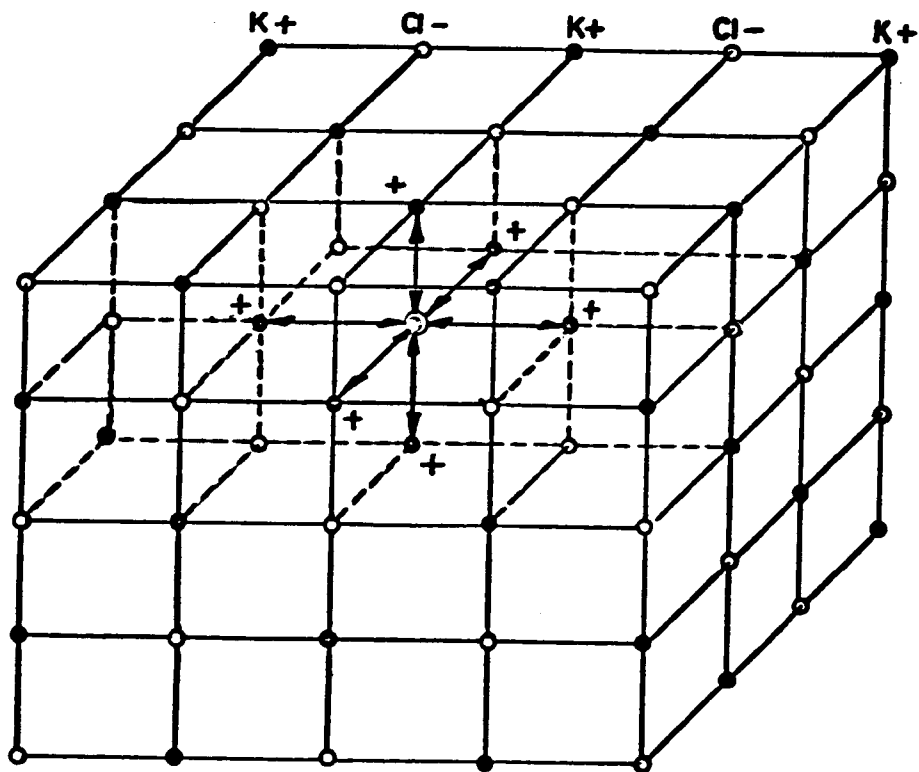


FIGURE FOUR
REPLACEMENT OF Cl^- ION BY H^- ION IN
 K^+Cl^- -LATTICE

model shown in figure 4, one may begin to understand the effect of primitive lattice disturbances caused by vacancies or interstitials as applied later to the ILS array.

Consider a displacement of one atom by either a heavier or lighter one, or, for purposes of ease of description, a displacement of an ion in an ionic lattice, such as KCl by hydrogen. In this case, the light ion (H^-) within the positive K^+ cloud has its own frequency of vibration (stretching frequency), with an optically active electric dipole moment. Because of the very localized nature of this defect, the additional vibrational modes decrease rapidly with distance from the defect (actually exponentially). However, if these defects are not localized but comprise many atomic sites as in ILS, the lattice motions for such a lattice substructure lead to standing wave modes, literally generating a strain field as electrons are moved into shared positions, depending upon the density of the molecular constituent and field applied. The lattice motions for such a lattice substructure lead to multiple standing wave modes because of the bonds on either side of the sub-lattice or multiple disturbance.

By representing the substructure by a single dimensional line leading to a standing wave of: $\Delta n = \Delta(0)e^{-i\omega t} \sin nkd$ (figure 5), because of the limitation L of the size of the sub-lattice, K is restricted to:

$$K = \frac{\pi}{L} ; \frac{2\pi}{L} ; \frac{4\pi}{L} ; \dots \dots \dots \frac{n\pi}{L}.$$

The solution for (A) vanishes for $n=0$ and $n=N$ (fixed points), and for points in between, yields a number $K = \pi/Ld$ independent modes.

This analogy between defect or sub-lattice excitation and bound lattice modes may help explain a number of the effects to be discussed connected with infrared vibration spectra of the ILS and the disordered system array.

Dislocations, in conjunction with junction breakdown caused by the stressed bonds, introduce interband energy levels, therefore allowing the electrons to move easily through a lowered field, thus allowing interband transitions to the conduction band. It is suspected that many dislocation space charge pipes or elements of similar nature, perhaps assisted by the electronic wave functions, account for the fast response and lack of hysteresis in the ILS array.

In further analysis, in a structure such as the ILS, a multitude of bonds, known as dangling bonds, are thought to exist, which are generally commonplace around and in the space charge pipe sites. These dangling bonds are in an excellent position throughout the structure to pick up shared electrons, thus creating a tremendous amount of strain or stress upon the inner bonds; therefore, the structure will also tend to purge itself of molecules of the gas constituent of interest when the molecular density is reduced or removed entirely from the vicinity of the sensor. This purging, or flyback as it may be called, occurs within 150 milliseconds in some cases.

Selection of Semiconductor Materials

Past experience at Thunder Scientific has indicated that transition metal oxide complexes appear to be the best for use in the construction of the ILS arrays. Transition elements, have partially filled d or f shells. Before describing the method to be employed to construct the ILS array, or configurations and transition complexes analyzed and employed, further discussion is required to better understand the semiconducting effects of transition metal oxides and their particular applications to this effort. Characteristics of the various transition metal oxides are quite interesting, in that it becomes rapidly apparent that various combinations display extremely varied electronic, ESR and vibrational spectra and that by very minute variance of the mix and process times, temperature and diffusion gases, the stretching frequencies may be manipulated rather precisely. Some of the various coordinate complexes can be made to take up an additional odd or even ligand very readily. Valence states, relative ionic radii, associated bond lengths, and stretching frequencies are extremely important in determining the final configuration best fitted for monitoring each gas constituent.

Ligand Field Theory

To gain a better understanding of the effects taking place at a molecular level, it is well to define and explore ligand field theory as it applies to the problem at hand. Ligand field theory is defined, in this sense, as the theory of (1) the origin and (2) the consequences, of the splitting of inner orbitals of ions by their chemical (gas) environments. The inner orbitals of interest in this case are the partially filled d or f orbitals, primarily the d. In this discussion, these splittings must be related to the forces

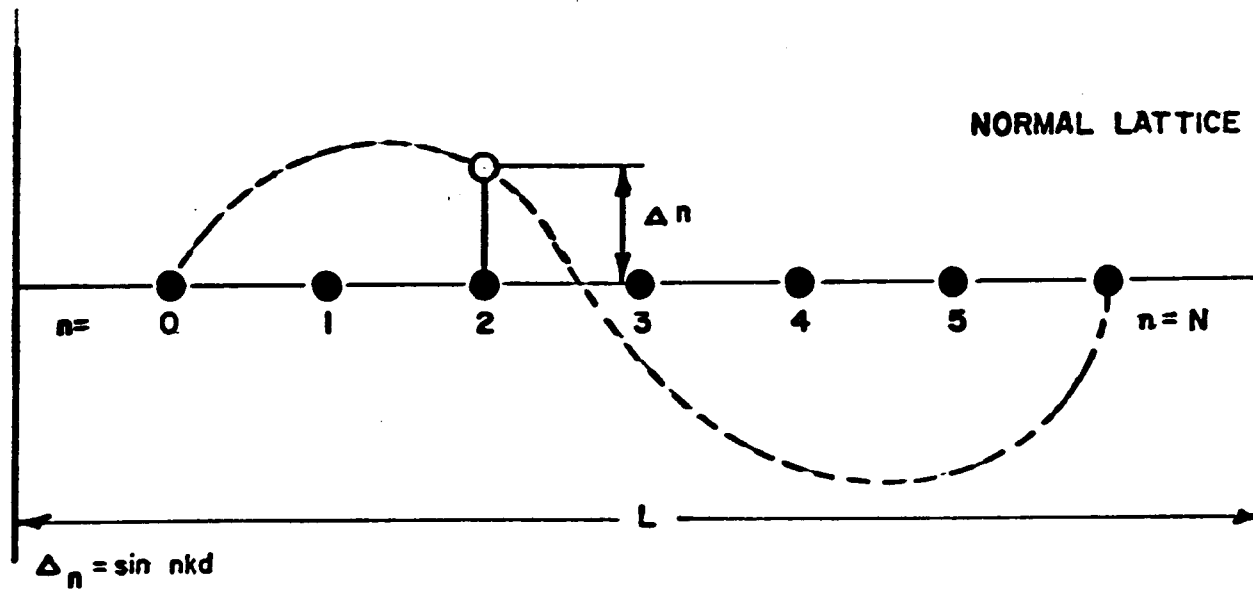


FIGURE FIVE
ONE DIMENSIONAL STANDING WAVE
OF n DEFECTS IN LATTICE

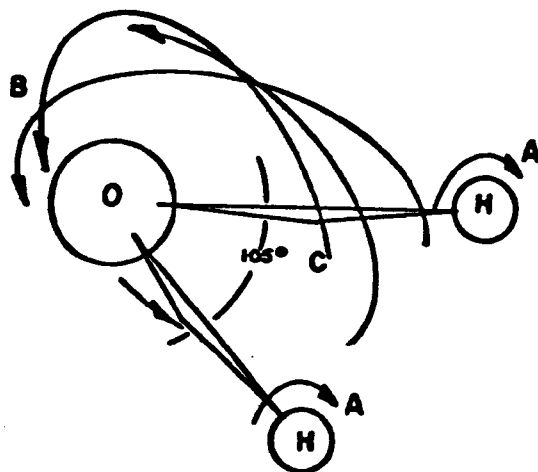


FIGURE SIX
 H_2O MOLECULE

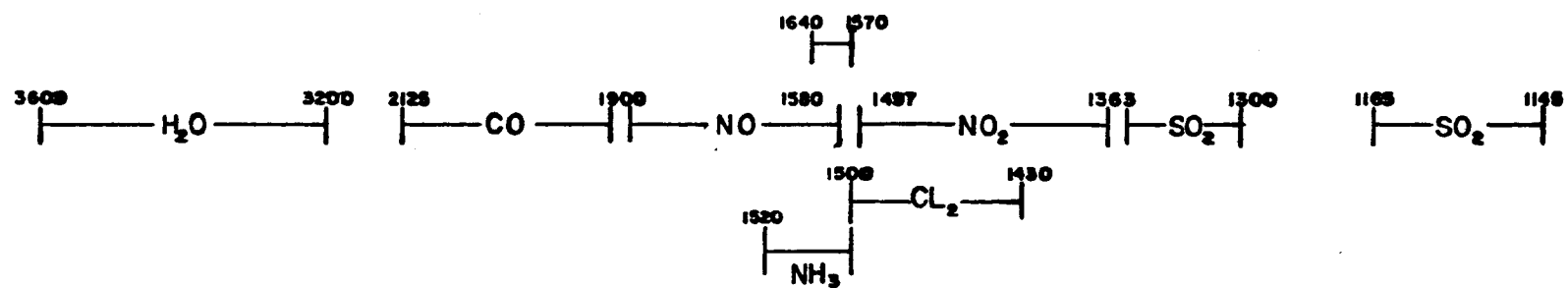


FIGURE SEVEN
FAR INFRARED STRETCHING
FREQUENCIES

involved. The ILS structure is not purely metal nor is it purely oxide, but rather a structure achieved by special processes, consisting of junctions containing both metal ions and oxide chains that contribute to the over-all spin and stress effects observed. (See figure 2).

Carbon Monoxide (CO)

Carbon monoxide, CO, is a pi acceptor ligand. Various pi carbonyls may also be associated. CO is a generally inert molecule and particularly adaptable for detection by the ILS array. Dipole moment studies indicate that the moment of an M-C bond is very low, about 0.5 D, which suggests that it is close to being electrically neutral as per Paulings law. CO has a bond length of approximately 1.128A. The CO molecule has a stretching frequency of 2145 cm^{-1} . If the carbonyl molecules are taken into consideration, a band would then exist of approximately $2125 - 1900\text{ cm}^{-1}$ in the far-infrared spectrum, providing both medium and strong spectra for detection resonance. Many combinations of carbonyls, and other atmospheric constituents, can be obtained in reactions that take place at normal atmospheric temperatures and pressures caused by the photochemical process.

Carbon Dioxide (CO₂)

Carbon Dioxide, CO₂, exhibits a stretching frequency from approximately 1570 to 1640 cm^{-1} . It shows some tendency to overlap NO; therefore, some discrete manipulation of stretching frequency was necessary to avoid confusion with NO. It was suspected that some latitude was available for this, due to the fact that the NO band is not continuous across the band of 1580 to 1900 .

Oxygen (O₂)

Oxygen, O₂, has an extremely broad band, exhibiting effects across the entire range.

Water (H₂O)

The water molecule has a stretching frequency of 3200 to 3600 cm^{-1} in the far infrared region, which are rated as strong resonances. Other minor resonances exist even into

the low infrared; however, these are weak to very weak and may be ignored. To better understand the complete theory of the ILS array, the water molecule presents an excellent opportunity in that it is relatively simple and readily accessible. The oxygen atom is bonded to two hydrogens in an arrangement expressed pictorially in figure 6. The separation of the hydrogens approximate, by present conceptual theory, an angle of 105° . Each hydrogen precesses at a given rate (A) and in conjunction with this momental precession, it is believed that a complex precession exists about O, as shown by B following through C and so on. These perturbations may be attributable to the anti-symmetric and symmetric O-H stretching mode at 1600 to 1650 cm^{-1} . In addition, quite a good deal of fine structure is apparent. Therefore, as the molecular density or moisture content of the atmosphere in the vicinity of the Brady Array humidity sensor changes, bonds are stressed as previously explained, thus causing a shift in volumetric resistance of the Array and subsequent change in readout voltage. Further direct explanation of the Brady Array bulk-effect semiconductor humidity sensor is contained in a recently published paper (see Appendix).

Material Selection

As previously indicated, most, if not all, first transition series metal oxides will, when processed and doped correctly, exhibit semiconductor phenomena. With proper processing, the resistance of resultant elements may be controlled over a broad range of as much as 10^{14} ohms/cm or more when using the ILS technique. Past processing indicates that the d-block elements with partially filled shells are d shells, 3d, 4d, or 5. These d orbitals project well out to the periphery of the atoms and ions so that the electrons occupying them are strongly influenced by the surroundings (the gas constituent) and in turn are able to influence the Fermi level and internal environment of the sensor substantially. The final selection of the precise transition elements, reactants, doping materials, processing temperatures and diffusion gases were determined during the program. As in the case of the previously developed bulk-effect Brady Array, these parameters were developed by a combination, in sequence, of mathematical analysis and empirical. Cut and try, X-ray and spectrum analysis of lattice and crystal structure had previously been performed upon the Brady Array in previous in-house research thus giving some idea of typical structure to be expected. The "cut and try" deals primarily with process times, temperature cycling rates and diffusion gas content and flow rates, following initial determinations of sensitivity to the gas constituent of interest.

Material Analysis,
Studies, and Selection

Initially, studies were instigated to determine proper bond lengths and radii, ionization potentials, melting temperatures, transition points, molecular weight, etc. of various oxides of metals to determine possible compatibility and/or sensitivity to the various gases desired to be monitored. Far infrared stretching frequencies were also taken into consideration and listed. Sources for these data are listed in the references contained in this report.

Based upon the above referenced studies, the following final test groups were selected for initial testing and analysis.

EPA Code #1

50% Fe₂O₃
30% ZnO
20% SnO₂

EPA Code #2

50% Fe₂O₃
40% ZnO
10% SnO₂

EPA Code #3

50% Fe₂O₃
20% ZnO
20% Co₂O₃
5% V₂O₅
5% SnO₂

EPA Code #4

50% TiO₂
50% V₂O₅

EPA Code #5

50% Co₂O₃
50% V₂O₅

EPA Code #6

50% Zn
50% Sn

EPA Code #16

TiO₂ + V₂O₅
+ Neodymium

Though a total of sixteen (16) test groups were initially mixed, it was determined that those listed above were most applicable based upon the previous studies.

Group Selection

To determine the applicability of each test group for use as a sensor, it was necessary to observe the structure of each when exposed to various firing schedules within the furnace. (an Astro Industries Series 1000) This was done by placing each raw material mix within ceramic boats and observing the effects achieved when the material was fired at 1500°C to 1550°C. If a disordered polycrystalline structure or tendency was noted, the material was marked for prototype sensor construction. Of the 16 test groups, those listed previously exhibited this tendency.

Sensor Construction

Each sensor was constructed by hand beneath a microscope upon glass cover slips. The material was mixed with a 95% - 6% mixture of beta terpinol and celulox acetate to form a binder.

The thus mixed material was then placed on a glass cover slip and formed, using a scalpel until a rectangular form was achieved measuring approximately 180 mils in length and 25 mils in width, with a depth of approximately six mils. Four mil platinum iridium electrodes were then embedded in the material equally spaced and the overall sensor shaped and flattened with the scalpel until of such a dried consistency to be picked up off the cover glass with the scalpel.

Sensor Firing

The completed sensors were then placed upon supporting mandrels within platinum boats and fired for thirty minutes at 1550°C. The boats were then removed and the completed sensor thermally lead bonded to a T0-5 type eight pin header.

Generally, it must be pointed out, at this stage in the development that a major portion of the process is one of "cut and try" including varying of temperature and diffusion gases.

As an example, the final configuration chosen for CO₂ was EPA Code #16. Here several gases were tried looking primarily for the largest crystal formation. All gas flows were flowed at the rate of 100 cc/min. The final gas chosen was a mixture of air and CO in a 75% air, 25% CO₂ mixture at atmospheric pressure.

In the CO sensor, it was determined that it functioned selectively to CO and discriminated against CO₂ when run at a current of 300 m.a. driven by a constant current module.

The material mix chosen due to the need for this higher current was EPA Code #1. This material when employed within the sensor showed no deterioration after long term running at this higher current.

Sensors were constructed of the various selected groups and designated as follows:

| | | |
|--------------|---|---------------------------|
| Test Unit #1 | - | EPA Group #1 |
| Test Unit #2 | - | 1st unit of EPA Group #4 |
| Test Unit #3 | - | 2nd unit of EPA Group #4 |
| Test Unit #4 | - | 1st unit of EPA Group #5 |
| Test Unit #5 | - | 1st unit of EPA Group #16 |
| Test Unit #6 | - | 2nd unit of EPA Group #16 |
| Test Unit #7 | - | 2nd unit of EPA Group #5 |

Tunneling electrodes were used to allow thermal lead bonding of the sensor into a small T0-5 can type enclosure. (See photo, Figure 9)

Electrical Configuration

An integrated circuit amplifier was constructed as a prototype to achieve zero offset and a span of 1 volt DC output. This amplifier was inserted into the circuit as shown in Figure 8. All sensors were initially tested with this basic breadboard.

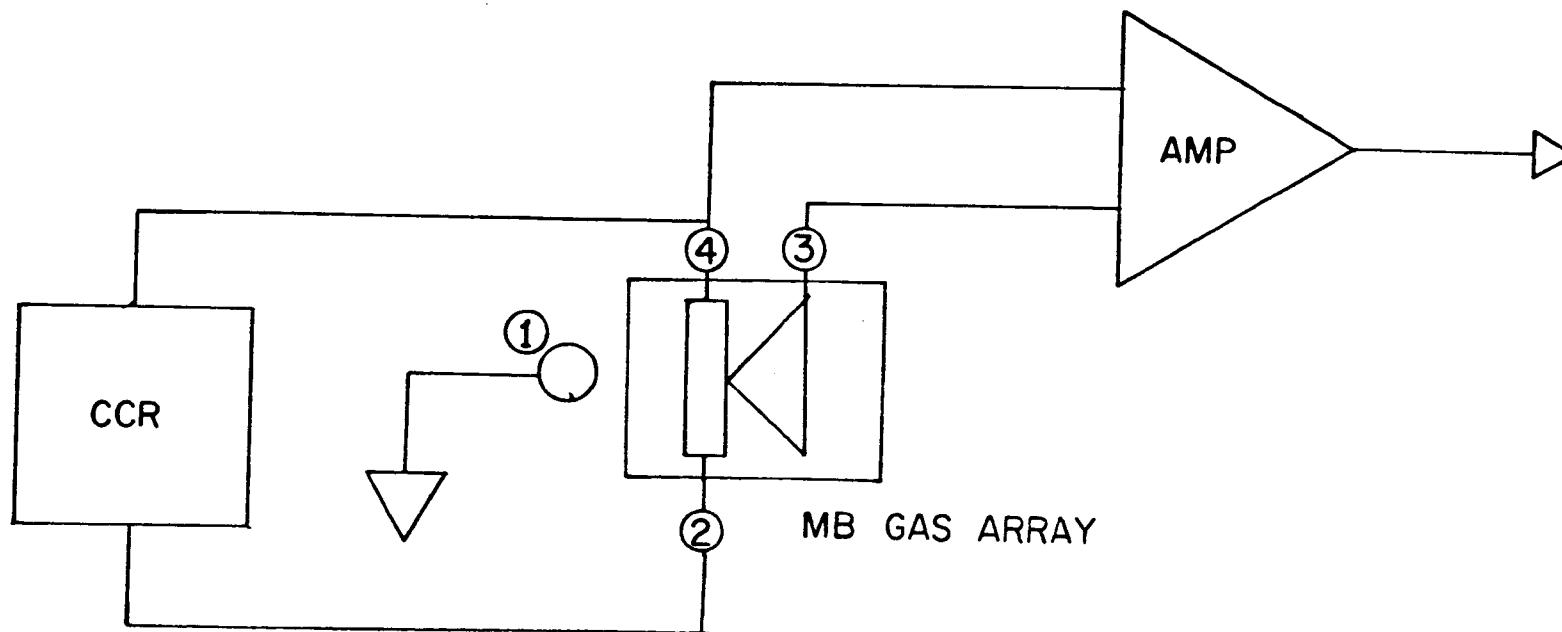
Initial Test Results

Of all sensors initially constructed, Test Unit #5, Test Unit #6 and Test Unit #7 indicated satisfactory sensitivity to CO₂ and were then further tested.

Test System Configuration

Initially an all glass test system was constructed as shown in the photograph to allow testing of the sensors in both gas and humidity environments. In addition to functioning as a mixing manifold for all gases in a precise manner, the system also provided means of injection of known amounts of moisture into the gases if so desired, allowing the capability of achieving better than $\pm 1\%$ accuracy in mixing ratio.

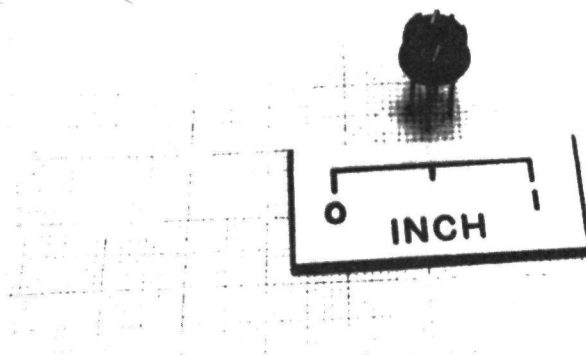
Precise accuracies of mixing ratio adjustment and flow were controlled by Matheson flowmeters with individual calibration curves for the various gas constituents. Mathematical computation allowed added precision when dealing with the various viscosities and specific gravities of the gases. Precision differential monometers allowed



NOTE: CCR = CONSTANT CURRENT REGULATOR

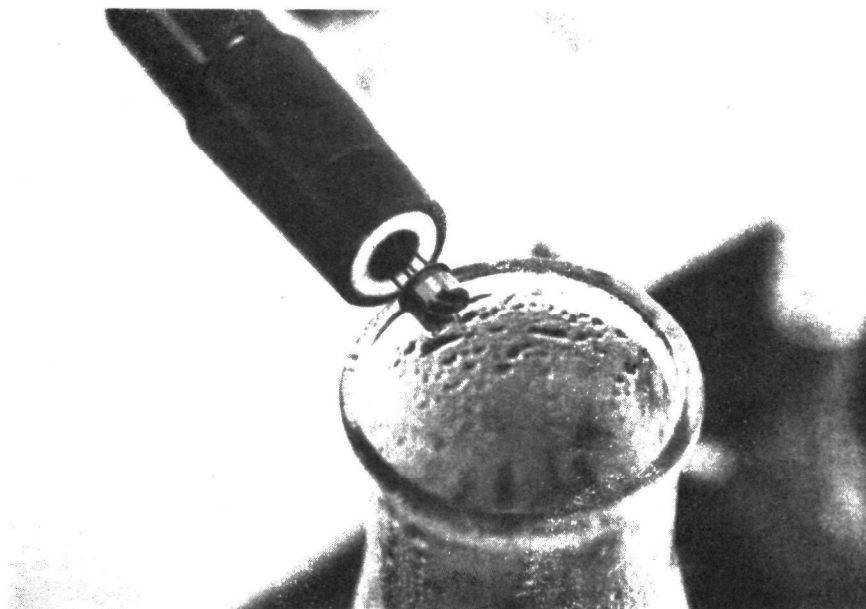
FIGURE EIGHT

BLOCK DIAGRAM EMISSIONS MONITOR
SIGNAL CONDITIONING CHANNEL



COMPLETED SOLID STATE
CO₂ GAS SENSOR

FIGURE 9



SENSOR IN ONE HOUR
STEAM EXPOSURE TEST

FIGURE 10

precise balance between the mixed constituents.

In initial testing for gas sensitivity and ranges, the test system was set up to allow use as a mixing manifold system only.

A standard Thunder Scientific Brady Array Humidity Sensor was first installed within the system to detect any moisture that might be leaking into the system. First tests indicated bad leakage, though all gases had been previously routed through two Ca SO₄ dessicators columns. Final source of leakage was traced to the tygon tubing used in the system.

Following this discovery, all tubing was replaced with a hard dense walled nylon tubing eliminating the problem.

The test sensor, Test Unit #7 was placed within the system and tests begun.

Initially dry nitrogen was used as a zero gas to establish a base. Gas flows were held to 100 cc/min. Temperature of the test chamber was continuously monitored and taken at each reading.

Test readout equipment consisted of a Fluke 853A Differential Multimeter, an 8300 DVM and an Esterline Angus Recorder.

The sensor was first checked for selectivity, the results obtained are shown in Figure 11. This recording was obtained by mixing in two Matheson type flowmeters. CO₂ was first vented into the system at 100% level and the amplifier adjusted to obtain a 1 volt DC output. The first recording shown in Figure 11 displays the response time of the Test Unit #7 with the chart running at 1.5" per minute. The second portion of the recording shown in Figure 1, displays the response to 100% CO₂ with the recorder running at 12" per hour. CO and O₂ were then vented into the system at 100% concentration, each time clearing the system with nitrogen. Selectivity of the sensor to CO₂ may be noted as a result.

Test Unit #5 was then installed within the system and the recorder run at 6" per minute. (See Figure 12) Here, due to the additional doping and material selection, it will be noted that the response time is considerably enhanced.

Test unit #5 was then operated in ambient air in live steam for one hour. (See Figure 16) (See Figure 9)

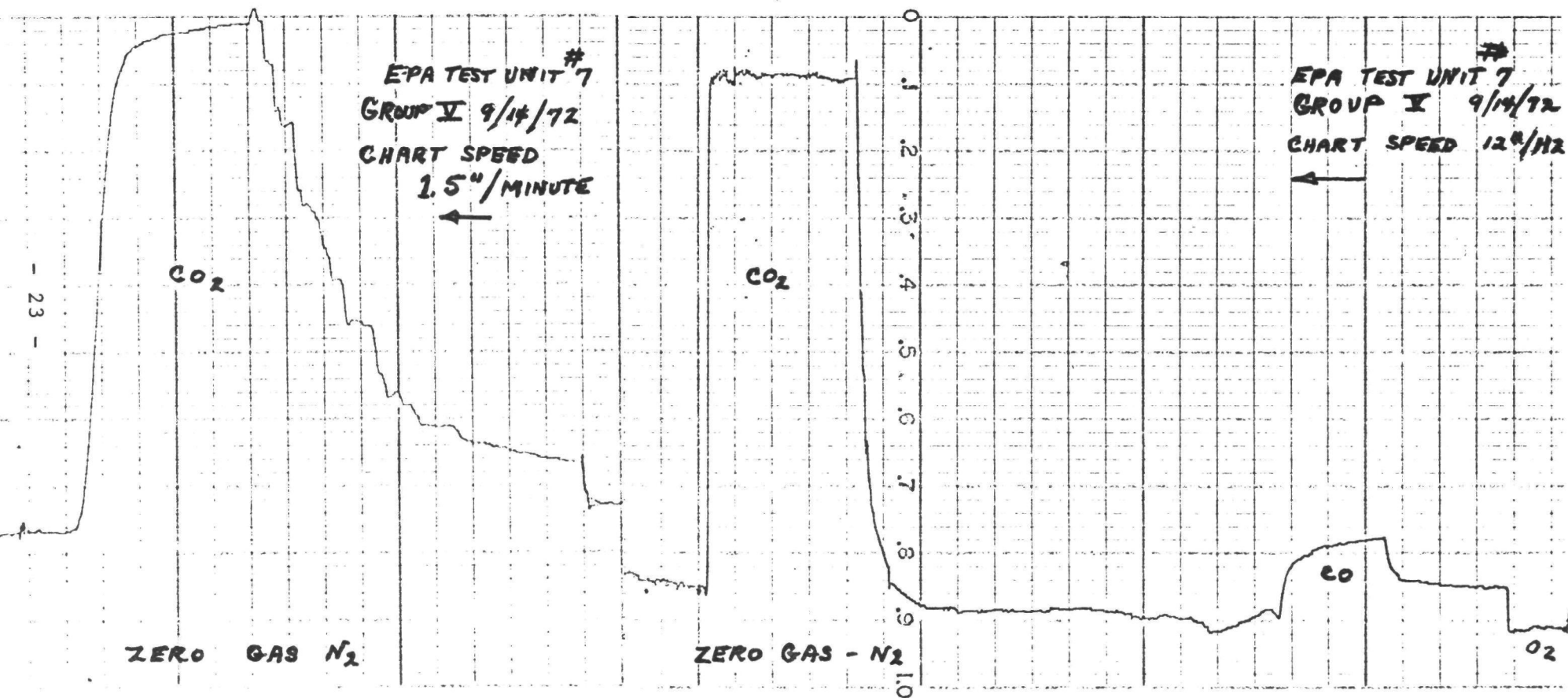


Figure
11

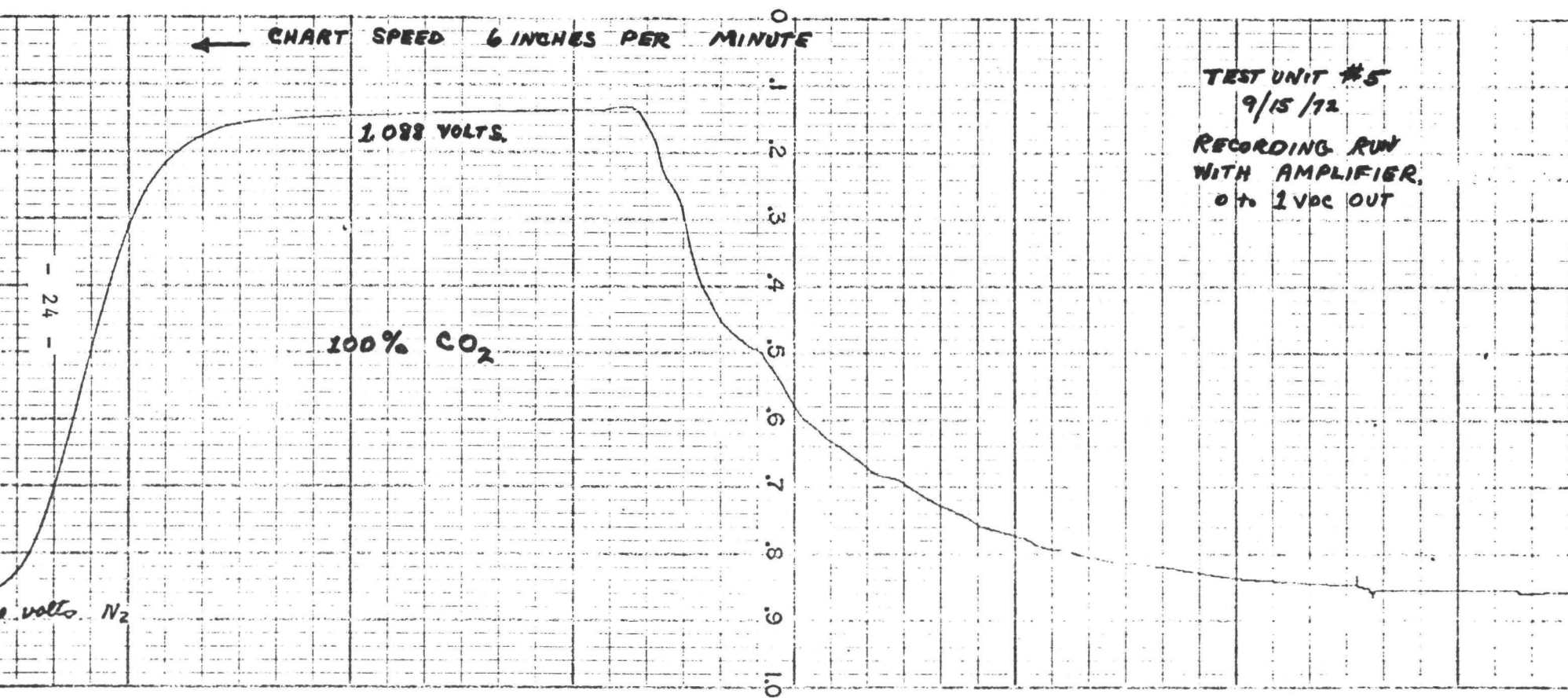
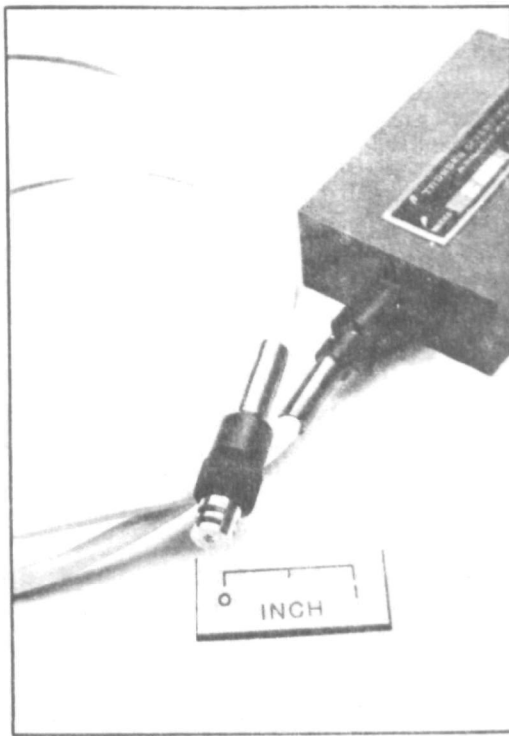
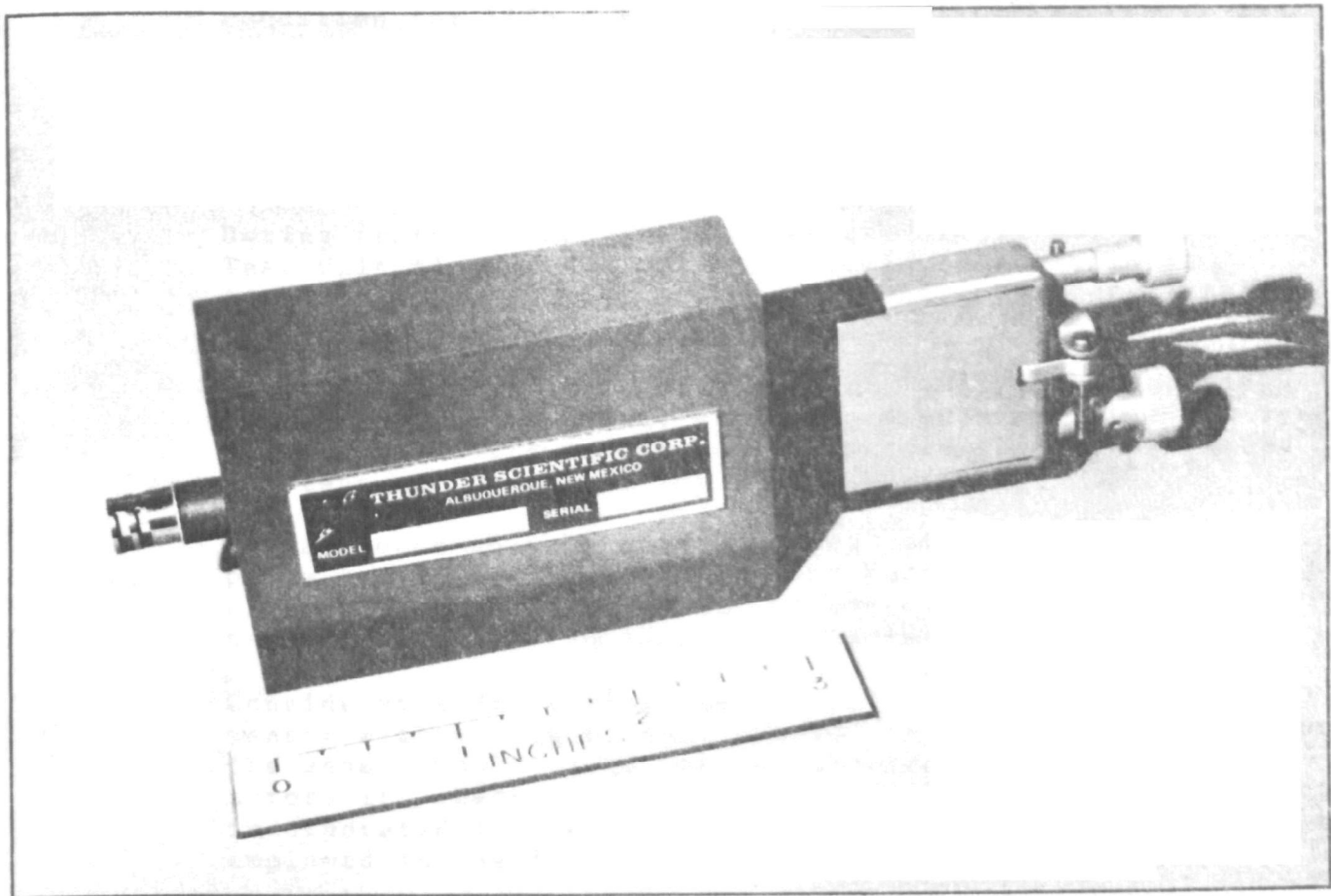


Figure
12



The SC-1020M signal conditioning module shown with the C-3A environmentalized cable and Brady Array



The SC-1020M signal conditioning module with Brady Array Model BR-101 humidity sensor

FIGURE 13

Following one hour in live steam, the recording shown in Figure 17 was run to determine any shift in calibration due to this exposure. It was noted that a slight shift of 44 m.v. occurred. Considering the stringent environment, this small amount of deviation was not considered serious.

A calibration run was made on Test Unit #6 and the recording shown in Figure 15 obtained. It will be noted that the sensor exhibits a near linear response to CO₂. These data are plotted and the curve obtained shown in Figure 14.

Of the test units run and tested, Test Unit #6 was selected for use in the Emission Monitoring System.

Life Tests on The CO₂ Sensor

The final sensor was installed at ambient in an operational condition for life testing. Prior to installation in the completed system, a total of 8000 hours was accumulated with no degradation in characteristics or output.

The CO Sensor

During tests of the various test groups, it was noted that Test Unit #1 of EPA Group 1 exhibited characteristic sensitivity to CO, i.e., response, etc. However, sensitivity to CO₂ was also noted.

The CCR, Constant Current Regulator, nominally supplying 20 m.a. to the CO sensor was changed to a variable CCR type generator and the output current across the sensor varied in steps as the output was evaluated.

It was found that apparent "tuning" of the sensor took place and as the internal current thru the sensor was increased, the sensitivity to CO₂ was eliminated, while the sensitivity to CO content was enhanced.

Considerable difficulty was experienced in clearing the CO sensor with nitrogen, once exposed to CO. It was found that the sensor would clear when a standard air mix was flowed across it. Because of this, a special "CO PURGE" valve was incorporated in the system. Test Unit #1 was selected to be employed in the final Emissions System for sensing of CO.

1.00

EPA TEST UNIT #6
GROUP 16
CALIBRATION 9/13/72

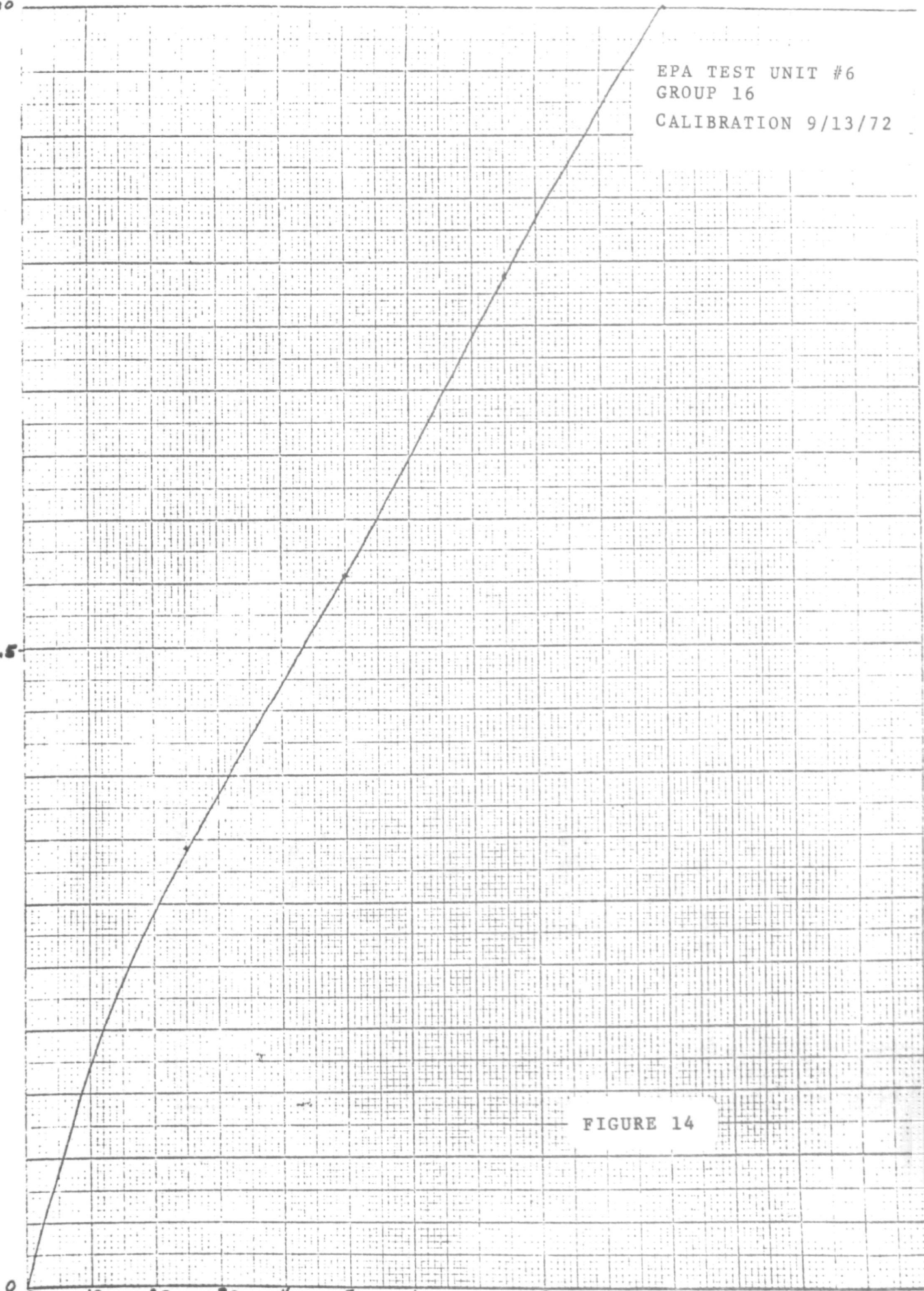
rs

0.5

0 10 20 30 40 50 60 70 80 90 100

CO₂ %

FIGURE 14



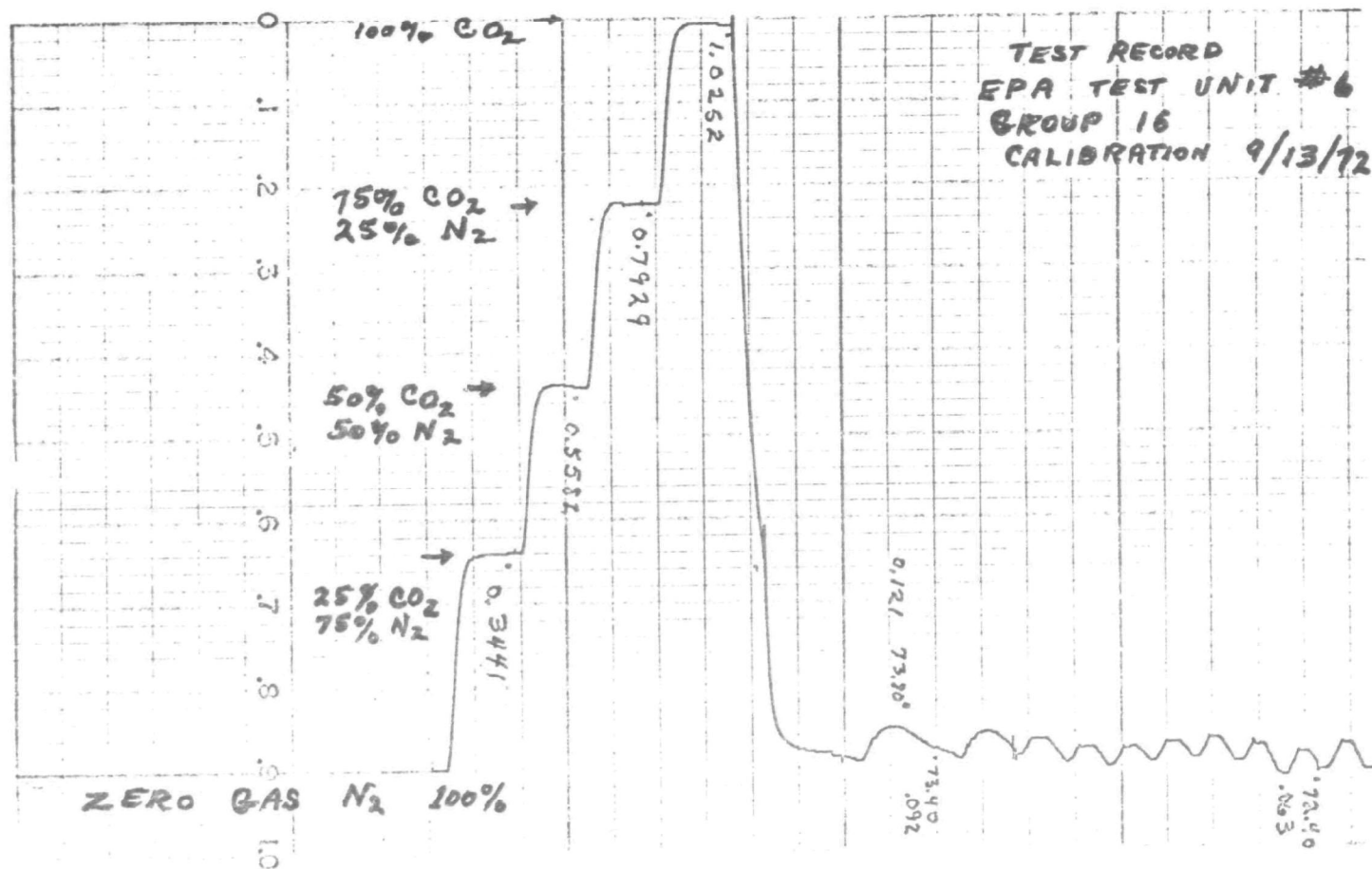


Figure
15

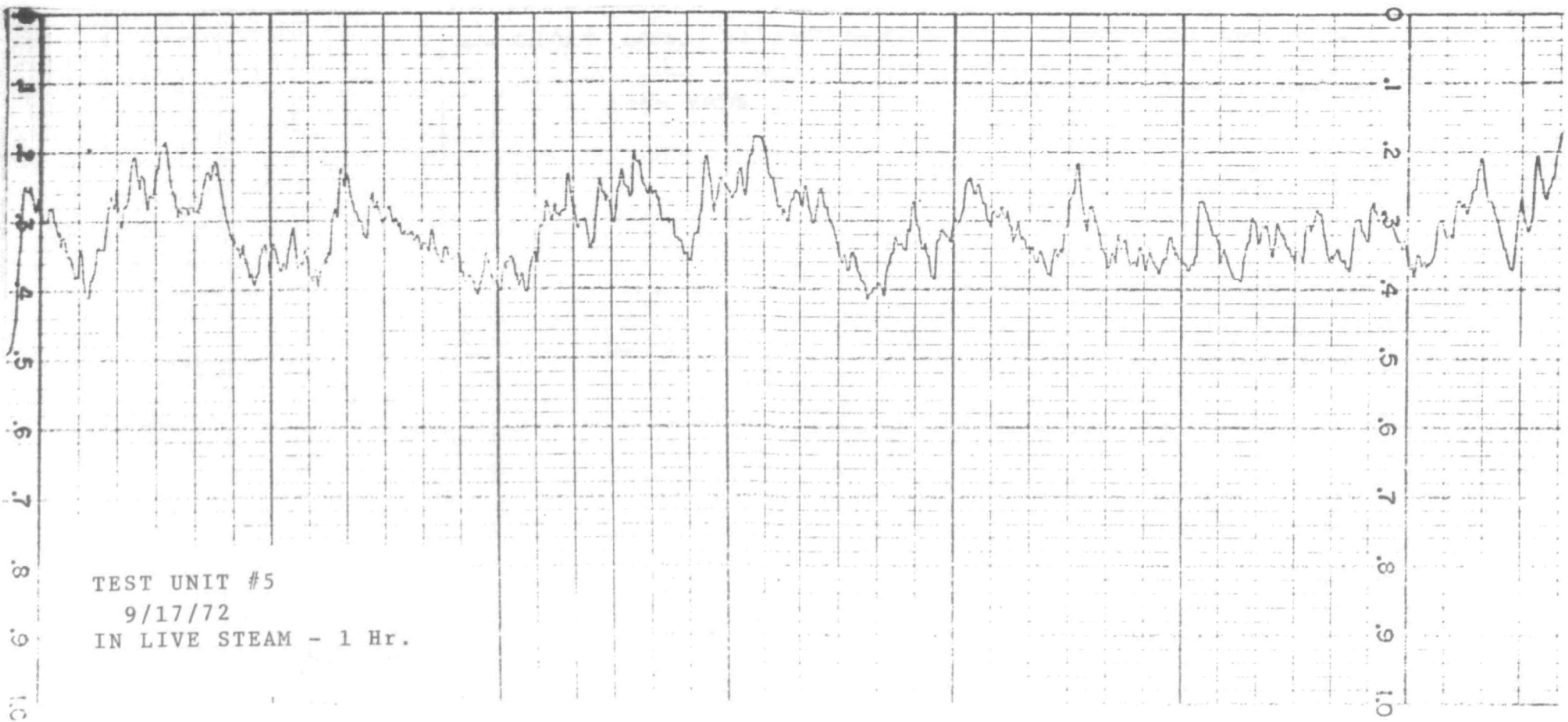


Figure
16

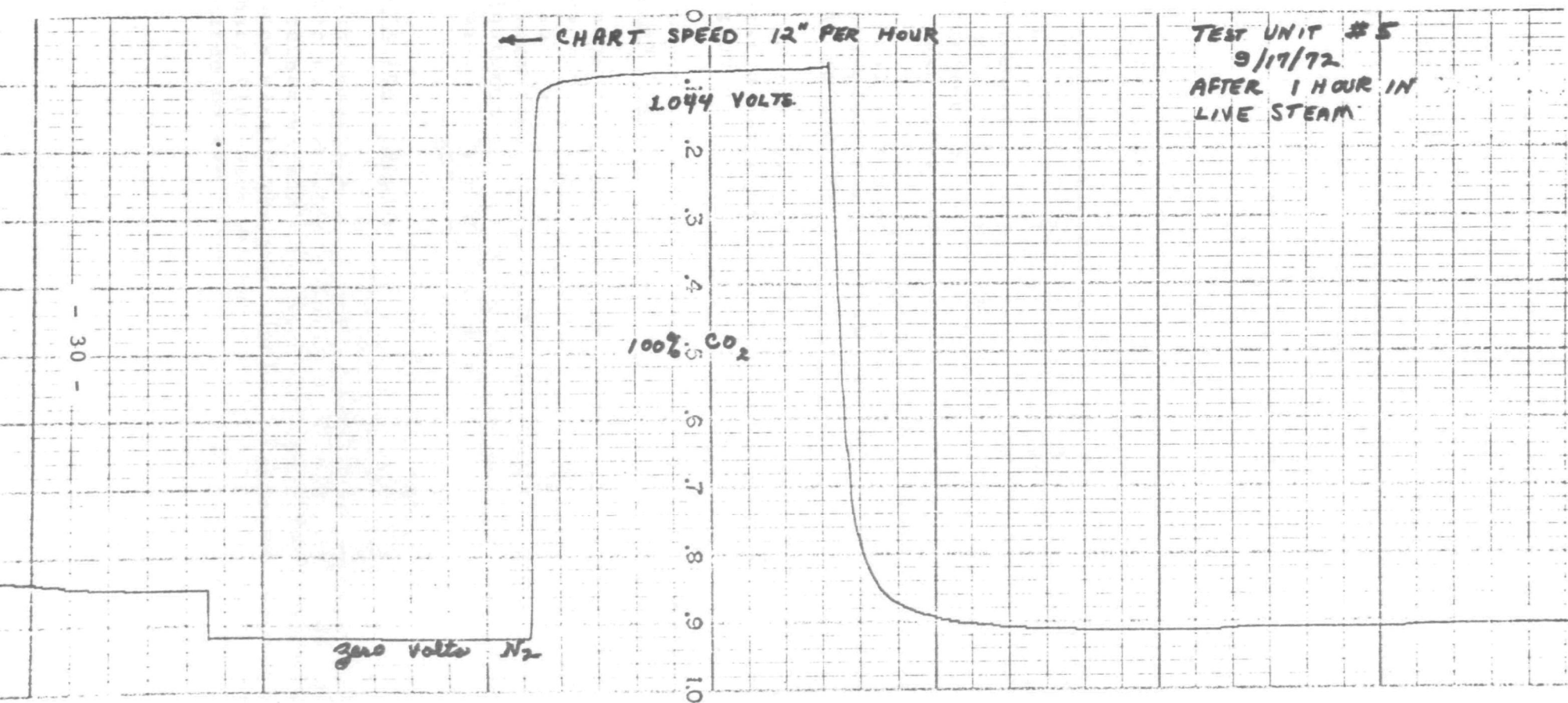


Figure
17

The O₂ Sensor

Considerable difficulty in the course of the program was experienced in obtaining a solid state oxygen sensor. It was finally determined that, though it appeared possible, with time, to obtain an oxygen sensor employing similar techniques, that a standard commercially available instrument would be incorporated for this measurement. A Beckman Model 715 Oxygen Analyzer was chosen in the course of evaluation.

The H₂O Sensor

The Brady Array Model BR-101 in conjunction with a standard signal conditioning module, Model SC-1020M-2 manufactured by Thunder Scientific Corporation was employed for measurement of water vapor present within the gas stream. This system has been employed by many in the field for measurement of humidity with a high degree of success over the past three years.

The Brady Array has a specified accuracy of $\pm 4\%$ RH, typical accuracy being better than $\pm 2\%$ RH. The range covered is 0% RH to 100% RH.

Due to its specific design, the sensor can be operated at elevated temperatures, i.e., in a heated sampling enclosure, ranging up to 160°F. (See Figure 19)

System Flow Transducers

Because it is necessary to maintain a reasonably consistent flow across the gas sampling sensors, a sensitive flow sensor was incorporated. This sensor, a Thunder Scientific Corporation Model WSIS-1000 allows measurement and precise adjustment of the gas flow within the system to 100 to 200 cc/min. (See photo in Figure 18)

Stack Temperature

Stack temperature is monitored and displayed on an analog meter on the front panel. A thermocouple and reference is contained within the sampling probe for monitor of temperatures within the gas intake. The probe is equipped with a back flushable micron filter with the back flush control located on the front panel of the switching module.

Stack Flow Rate

Initially the Model WSIS-1000 was investigated for use in determining stack velocity, however, it was found that the extreme temperatures that could be encountered within the stack prevented use of this device. Though Stack Flow Rate is displayed on the front panel, no satisfactory means was discovered in the course of the contract to monitor this parameter accurately.

The Emission Measurements Monitoring System

The Model EMMS-100 Secondary Emissions Monitoring System was developed in the course of the contract to provide a compact, but complete, self contained monitoring system for monitor and recording of levels of CO₂, CO O₂, H₂O and temperature in stack gases of power plants or in other emissions generating facilities.

The Switching Panel controls all gas switching and routing within the Gas Sampling System and provides signal conditioning and control for all transducers in the system.

System Components

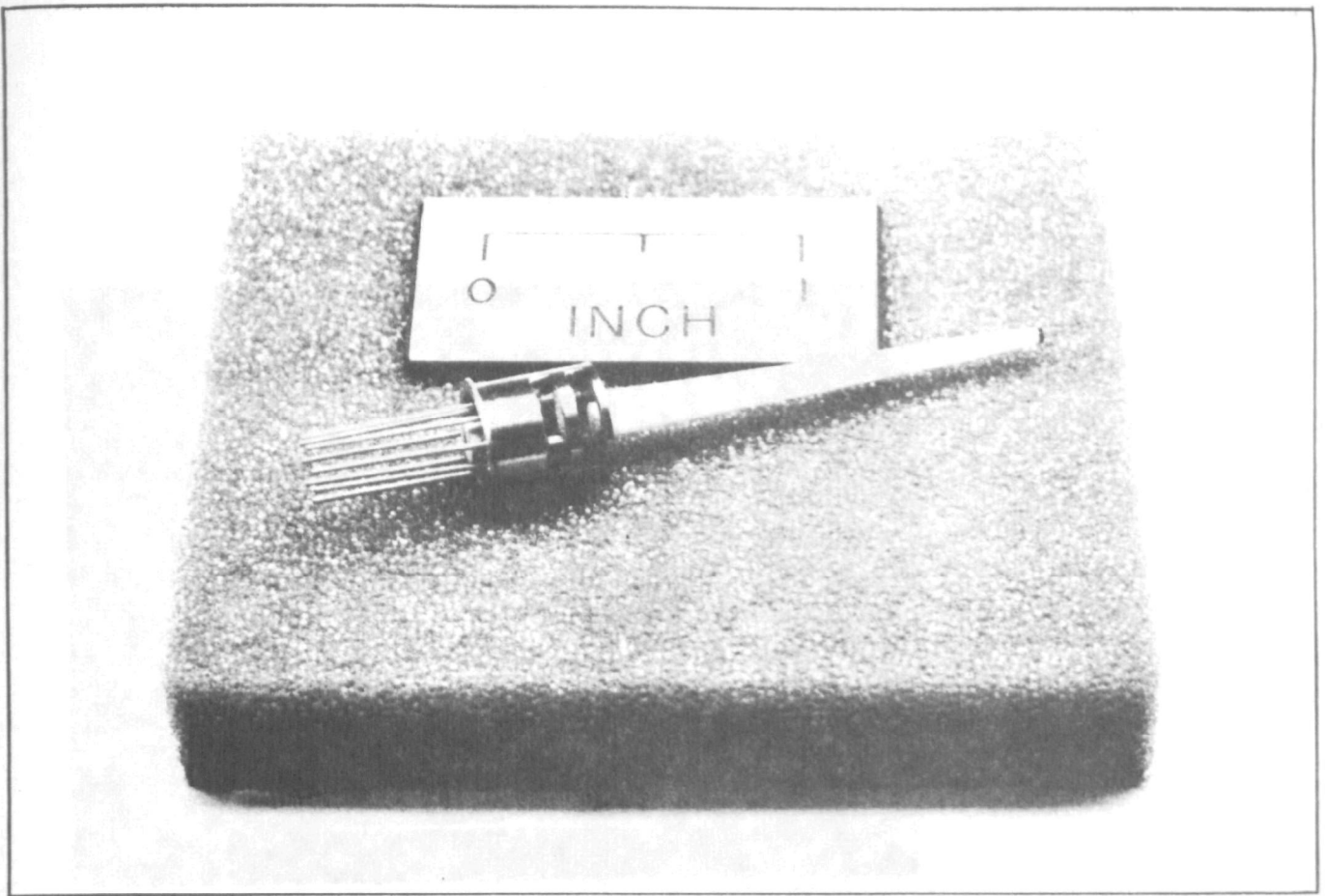
The system is constructed with 1/4" stainless steel tubing. All dryers, traps, sensor mounting blocks, etc. are constructed of stainless steel. All valves are electrically actuated directly from the front switch panel. Figure 19

A heated enclosure is contained in the top of the gas sampling system to maintain a preset temperature upon all critical components. Though the solid state sensors exhibit no sensitivity to water vapor, it was desired to maintain the system at a low level of relative humidity. This is accomplished by a proportional controller designed to allow adjustment of system heat from ambient to a maximum of 160°F.

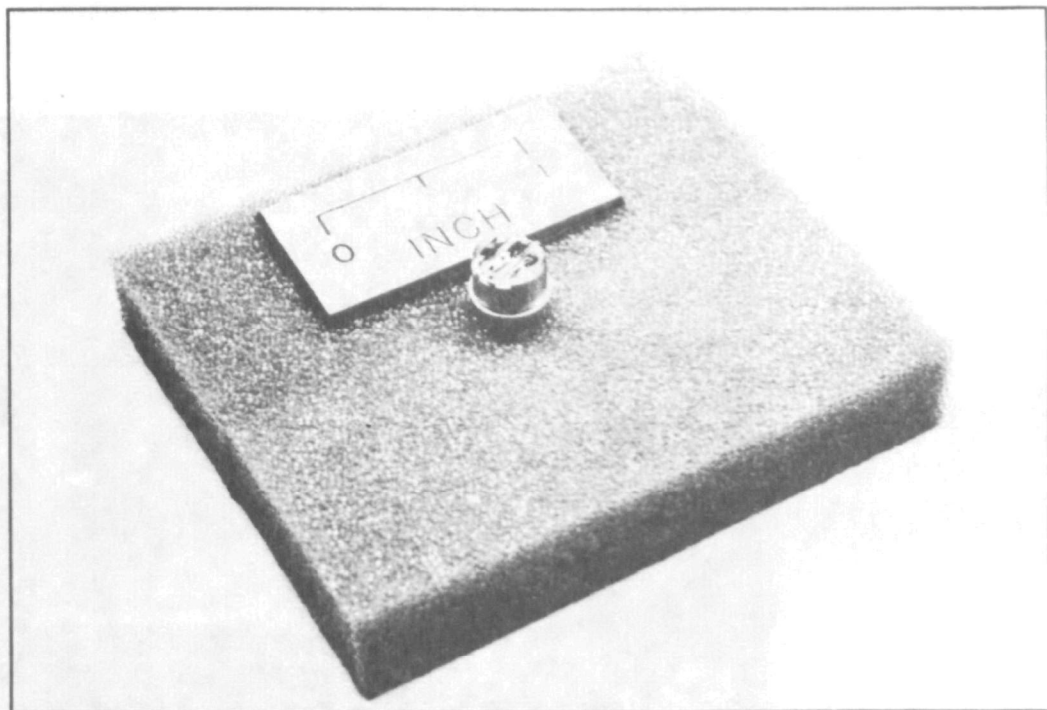
Switching

All switching is accomplished from the front panel of the switching module as shown in the photo. Figure 20

Switches are of the "push on" "push off" variety. All switches are labeled and back lighted.



WSIS-1000 FLOW VELOCITY SENSOR

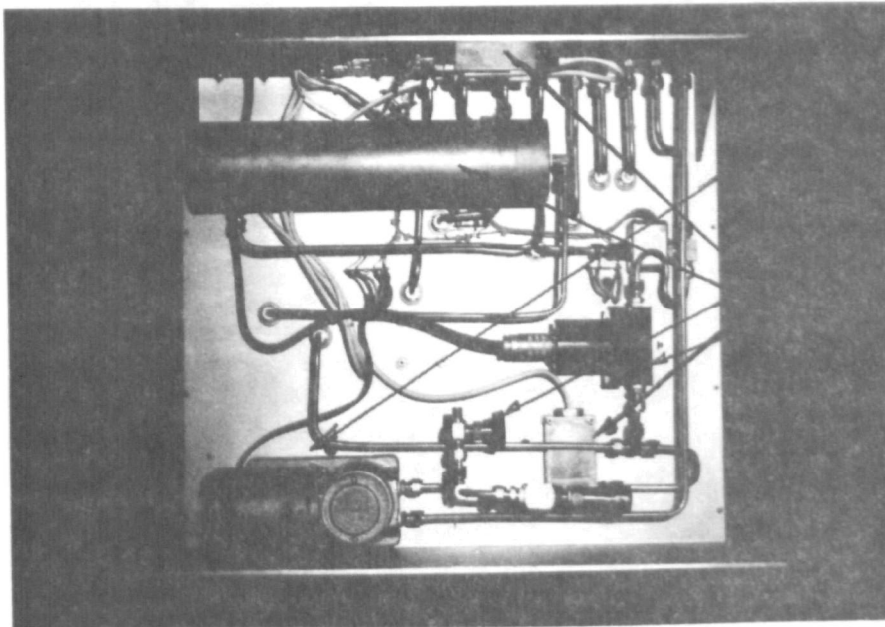


LOW PROFILE BRADY ARRAY SENSOR

FIGURE 18

GAS SAMPLING SYSTEM

BOTTOM VIEW



PUMP

SYSTEM VELOCITY
SENSOR WSIS-1000

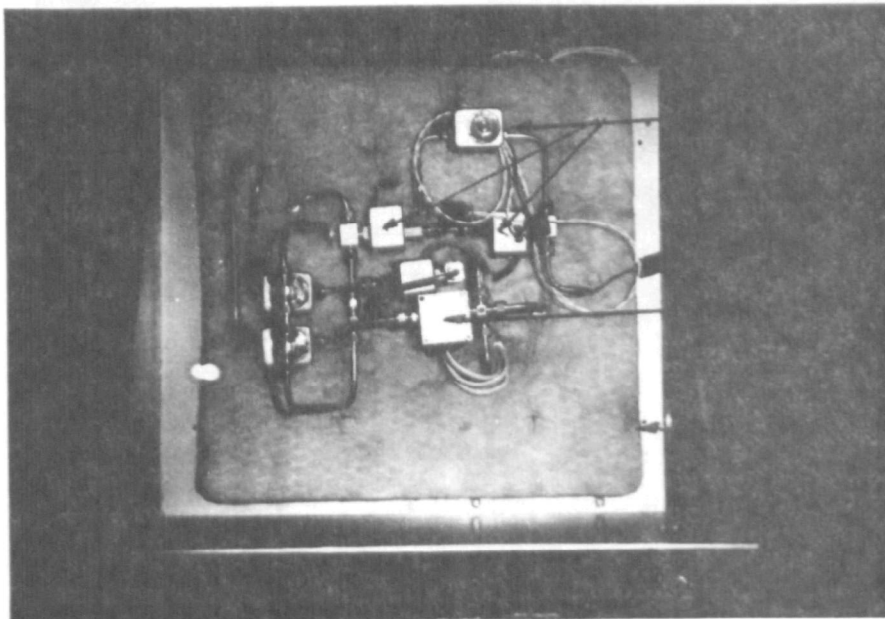
SYSTEM FLOW VALVE

O₂ SENSING HEAD

FILTER FLUSH
COMPRESSED AIR
FILTER

H₂O SIGNAL
CONDITIONING

TOP VIEW (HEAT SHROUD REMOVED)



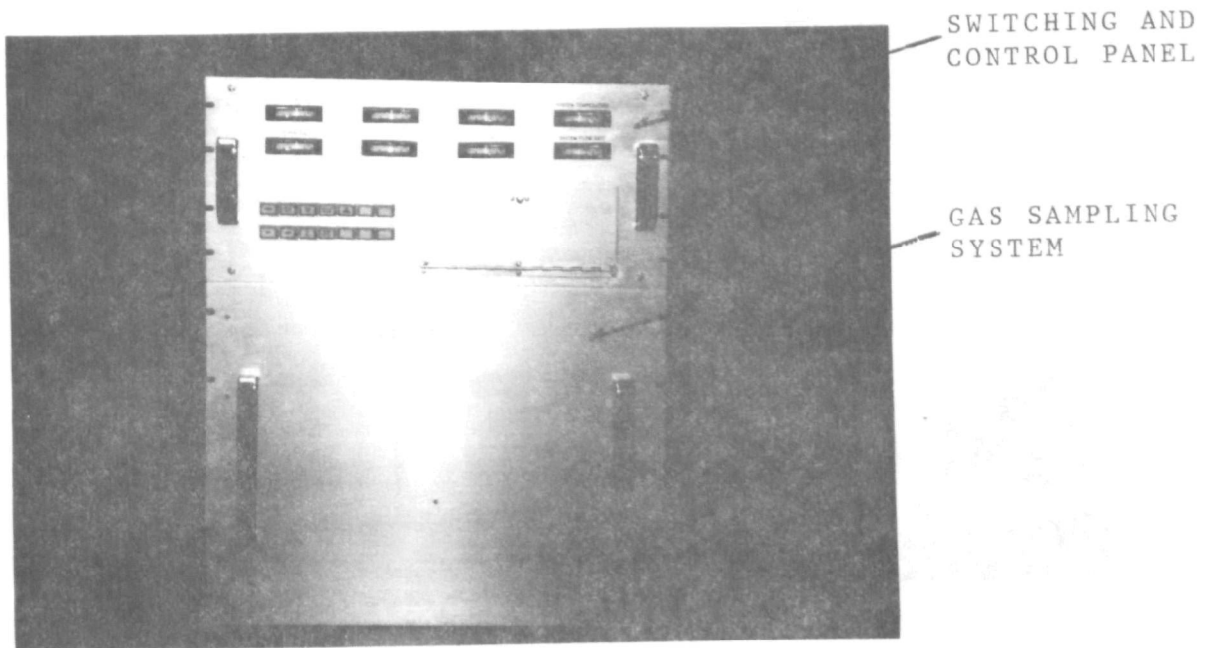
SYSTEM CONTROL
VALVES

CO₂, CO, & H₂O
SAMPLING CHAMBERS

GLASS FIBER
INSULATION

FIGURE 19

COMPLETE SYSTEM



SYSTEM SWITCHING AND CONTROL PANEL

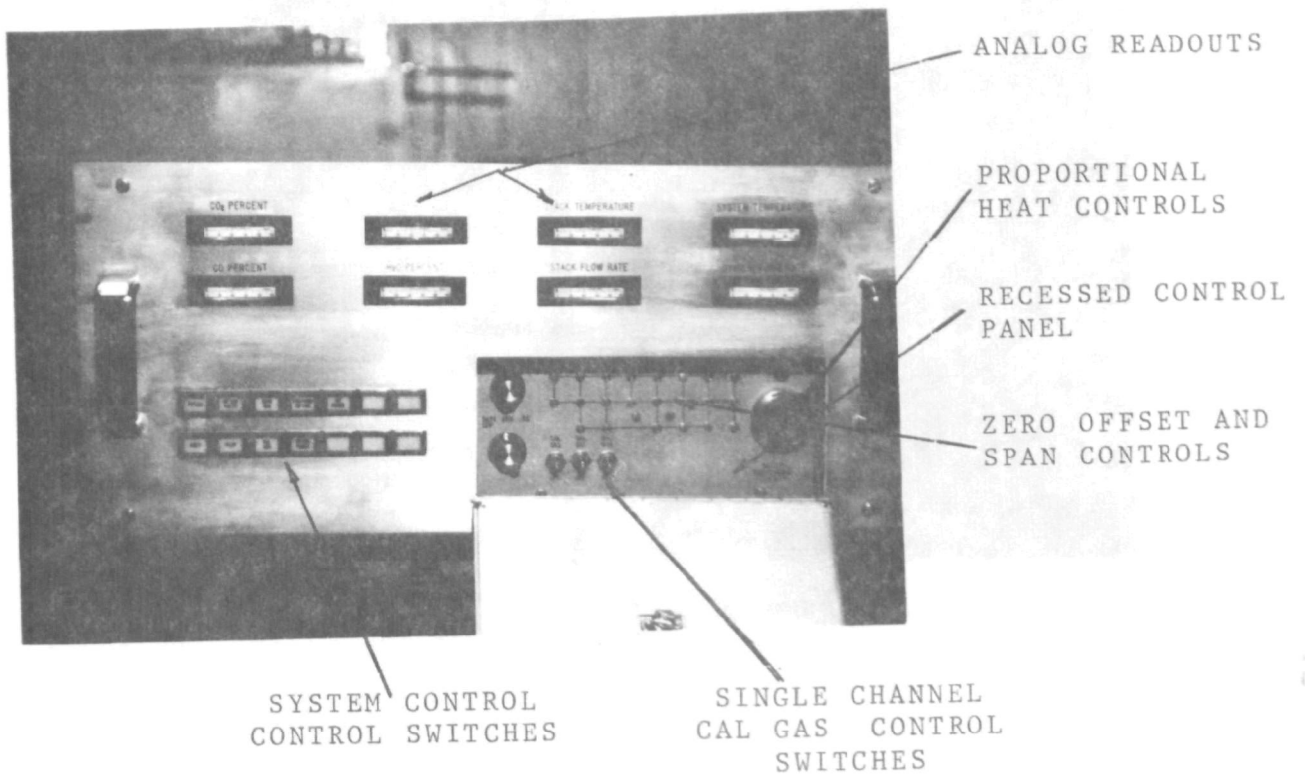
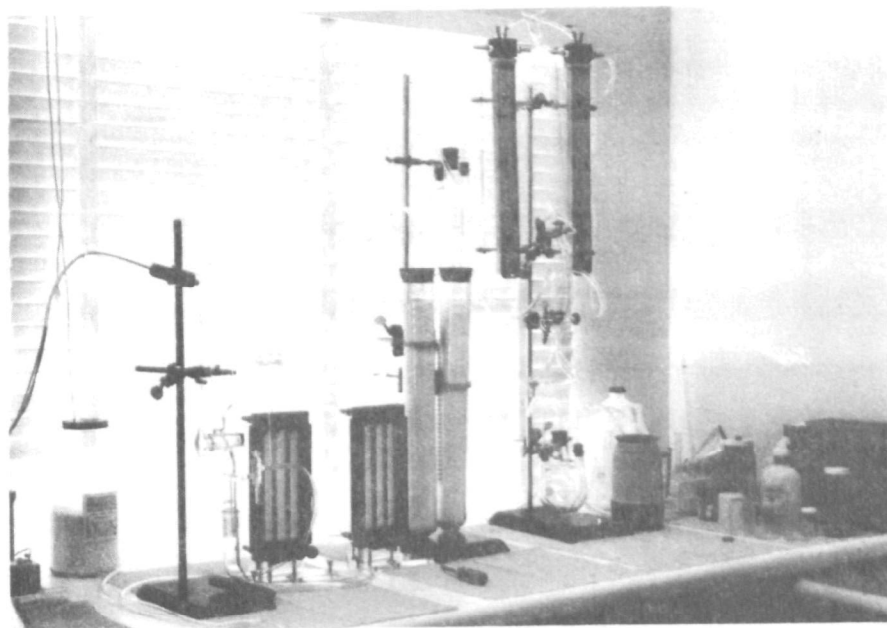
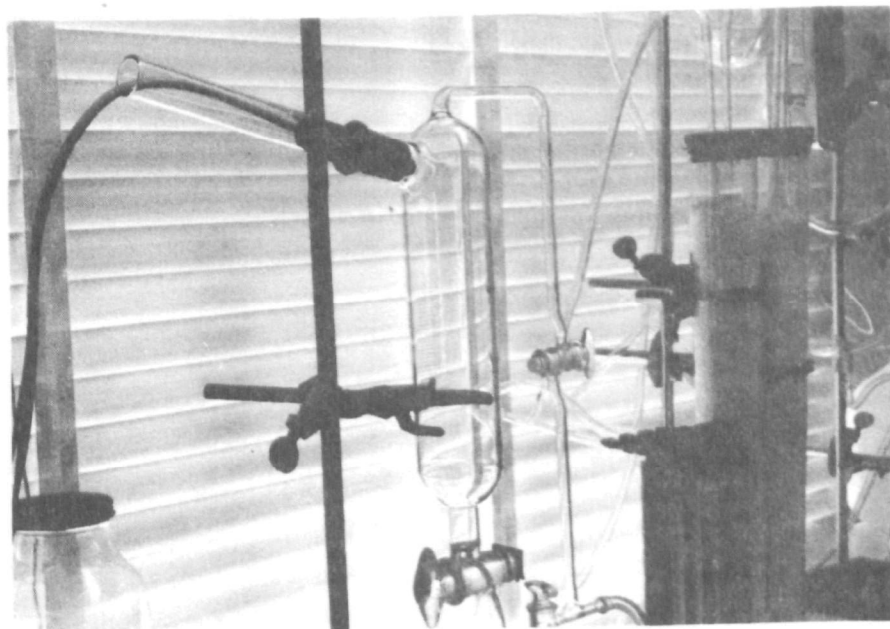


FIGURE 20



ATMOSPHERIC GENERATOR SYSTEM



TEST CHAMBER

Power

Power is controlled by a back lighted switch on the front panel labeled "POWER"

Intake Valve

The "INTAKE VALVE" switch controls the intake valve at the input of the gas system.

Zero Gas

The "ZERO GAS" input at the rear of the system is controlled by a front panel switch labeled "ZERO GAS".

Computer on Line

The "COMPUTER ON LINE" switch, located on the front of the switching panel switches the 0 - 1 VDC outputs of all electronic modules to a connector available at the rear of the chassis.

CO Purge

A switch is provided to allow purging of the CO sensor with air following each reading.

Filter Flush

A switch is also provided for back flush of the sampling probe and filter with compressed air.

Other control functions include system heat, pump, Cal Gas.

Sub Panel Control Functions

Control functions within the sub panel include zero off-set and span adjustment for all electronic modules for calibration adjustment. In addition, the proportional heater control, O₂ analyzer controls and individual channel Cal Gas switches are included within this panel.

Conclusion

It has been determined in the course of the program that viable and useful solid state semiconductor sensors can be constructed and tuned to accurately and selectively measure CO₂, CO and H₂O percentage ranges within a closed gas sampling system.

That a reasonably small compact gas sampling and control system can be constructed to allow efficient use of the concept.

EPA SYSTEM GAS FLOW

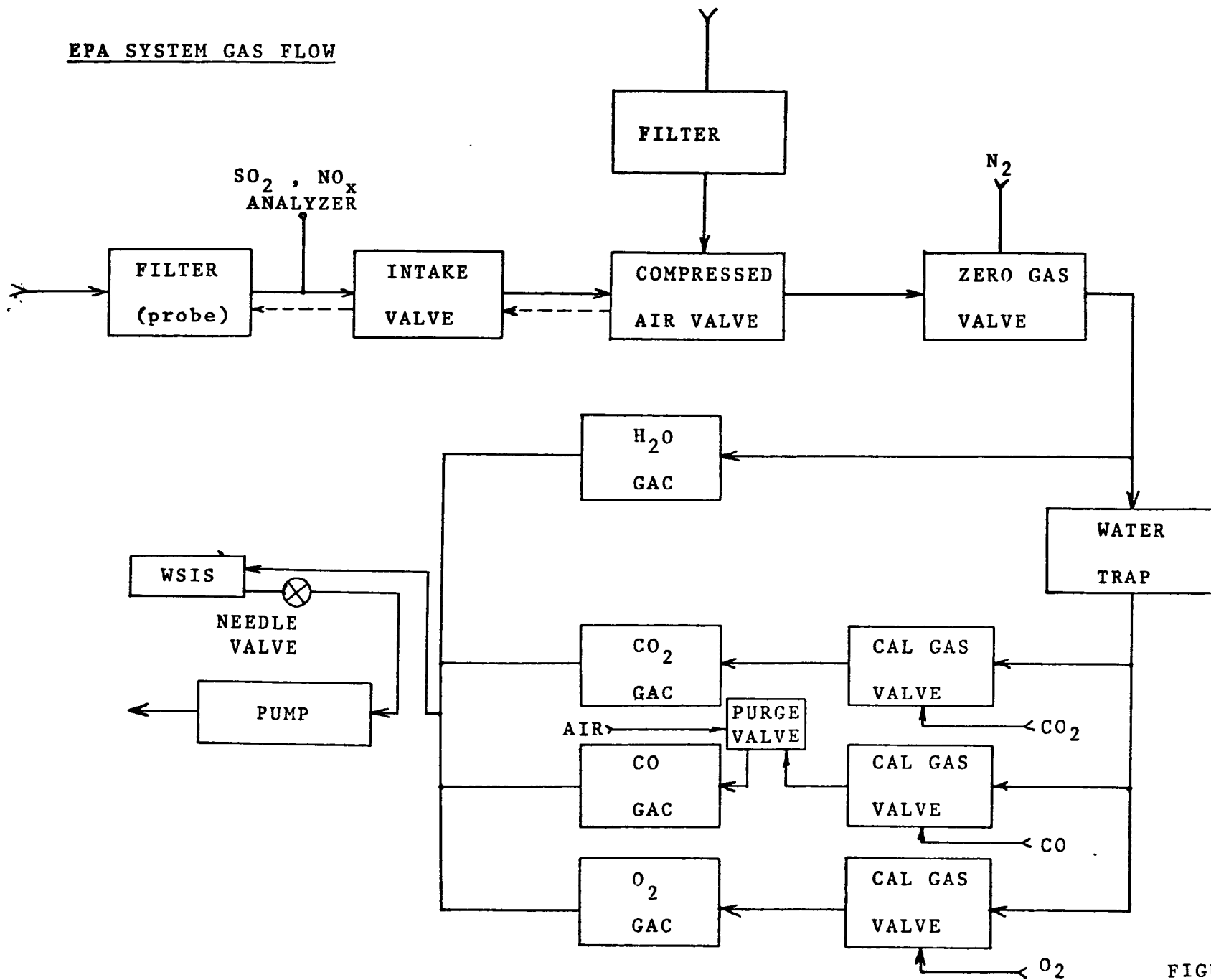


FIGURE
TWENTY-ONE

- 40 -

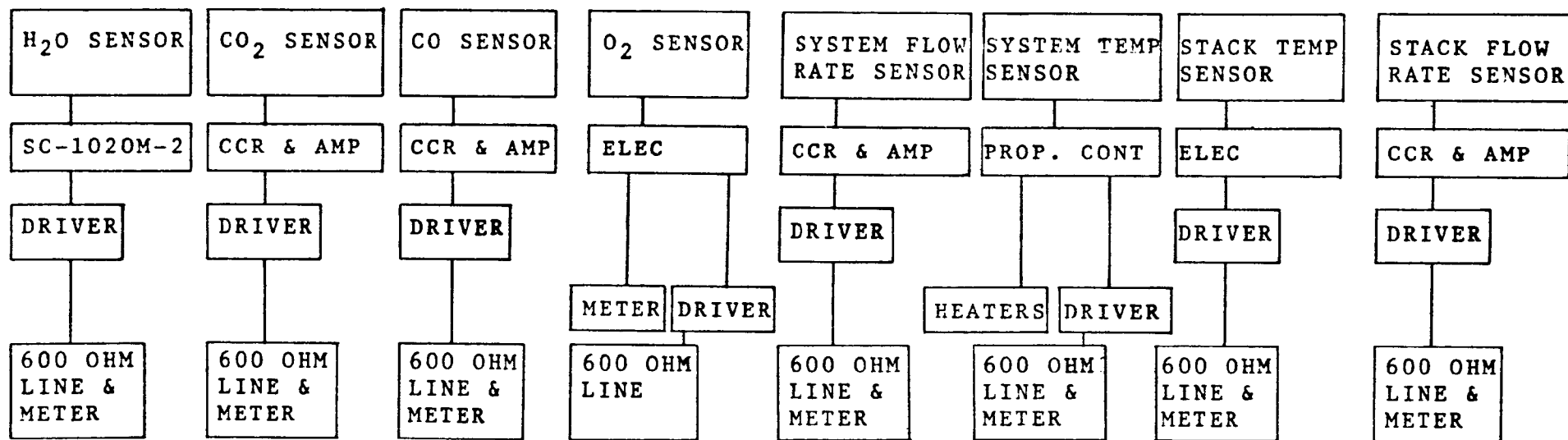


FIGURE TWENTY-TWO
ELECTRONICS FLOW CHART

References

1. Mott, N. F.: "Electrons in Disordered Structures," Advances in Physics (British), vol. 16, pp 49-144, 1967
2. Gubanov, A.: "Quantum Theory of Amorphous Semiconductors," Consultants Bureau, New York 1965
3. Ovshinsky, S. R.: "Reversible Electrical Switching Phenomena in Disorder Structures," Phys. Rev. Letters, vol 21 #20, pp 1450-1453, 11 Nov 1968
4. Morin F. J.: "Halides, Oxides and Sulphides of the Transition Metals," J. Appl. Phys. suppl vol 32 #10, pp 2195-2197, October 1961
5. Ferraro, J. R.: "Low Frequency Vibrations of Inorganic and Coordination Compounds," Plenum Press, New York, 1971
6. Sze, S. M.: "Physics of Semiconductor Devices," Wiley - Interscience, 1969
7. Leighton, P. A. (Stanford Department of Chemistry): "Photochemistry of Air Pollution," Academic Press, New York, 1961
8. Sheehy, J. P., Achinger, W. C., Simon, R. A.: "Handbook of Air Pollution," Environmental Health Series, U. S. Dept. of Health, Education and Welfare National Center for Air Pollution Control, Durham, N. C.
8. Bennewitz, Paul F.: "The Brady Array - A New Bulk-Effect Humidity Sensor," Society of Automotive Engineers #730571 May, 1973